Chapter

Toxicologic Characteristics of Nanodisperse Manganese Oxide: Physical-Chemical Properties, Biological Accumulation, and Morphological-Functional Properties at Various Exposure Types

Nina Vladimirovna Zaitseva
and Marina Alexandrovna Zemlyanova

Abstract

Nanosized manganese oxide has excellent prospects. Some data imply that its particles can be toxic when introduced in various ways, and it requires further examination of this nanomaterial. The authors conducted research of nanodisperse MnO_2 water suspension at intragastric, inhalation, and skin-resorptive introduction into small rodents and obtained profound characteristics of its toxic effects, determined target organs and revealed dose-dependent effects. The substance was characterized with acute toxicity, and its bioaccumulation under long-term exposure caused morphofunctional disorders in brain, lipid peroxidation activation, and lower antioxidant system activity. The authors detected vessel hyperemia, subarachnoid hemorrhages, brain edema with perivascular and pericellular spaces dilatation, nerve fiber demyelinization, and focal dystrophic changes in vessels endothelium. After a long-term introduction in doses from 0.25 to 2.5 mg/kg, oxidizing-antioxidant imbalance occurred, neurotransmitters and electrolytes balance was violated, and there was also brush border epithelium insufficiency. Nanodisperse MnO_2 water suspension in doses equal to 2.5 and 0.25 mg/kg at intragastric introduction into Wistar rats did not have embryotoxic or teratogenic effects. It did not have any mutagenic effects in doses equal to 10.3 and 5.15 mg/kg or gonadotoxic effects either when introduced into Wistar male rats in doses equal to 10.3–5.15 mg/kg via gastric tube.

Keywords: nanodisperse magnesium oxide, toxicity, acute exposure, chronic exposure, long-term effects, inhalation and oral route

1. Introduction

Nowadays, one can see rapid growth in worldwide development and commercialization of nanoindustries and nanotechnological products in overall

production chain; such products and technologies are considered to belong to a market segment of new technologies (the sixth technological structure) [1]. As per US Congressional Research Service experts assessment, world market of finished products and goods containing nanocomponents and nanomaterials now amounts to more than 1 trillion US dollars; it comprises more than 800 consumer goods produced with the use of nanotechnologies; by 2020, more than 15% of overall goods output in the world will be produced with the use of nanodevelopments, and the volume of this market in various sectors will be equal to more than 3 trillion US dollars. Aggregate volume of investment into scientific research and start-ups related to nanotechnologies received from various sources worldwide is estimated to amount to almost 20 billion US dollars. Annual nanoindustries market growth is expected to reach 20–30% [2]. In experts' opinion, nanoindustries and nanotechnologies (together with other technologies) are already facilitating transfer to new technological structure based on renewable energy sources, intellectual power engineering technologies, construction of completely new energy-efficient buildings, hydrogen technologies application, electrical and hybrid vehicle creation, 3D printer design and implementation, etc.

Nowadays, nanoclusters evolve quite intensely all over the world (more than 1700 cluster organizations in 260 European regions) and in Russia (more than 330 participating organizations). World market segments of nanomaterials develop as their commercial use in such key spheres as aerospace, health care, biotechnologies, power engineering, electronics and IT, processing industries, and consumer goods sector, grows rapidly [1, 3]. All this becomes apparent in the attitudes the European Union (EU) has toward the matter, declaring that nanotechnology is one of the Key Emerging Technologies 2020 Strategy. Its enormous potential for innovation has fostered large investments in developing new consumer products and industrial applications. The outlooks for a rapid growth in the sector have raised not only hopes and high expectations, but also societal concerns about the adequacy of nanotechnology regulation. Indeed, despite their clear benefits, engineered nanomaterials pose environmental and health risks [4].

All these processes prove the necessity to systematically examine potential dangers and threats for human activity, which are related to large-scale spread of nanotechnologies and nanobiotechnologies. In spite of all their undeniable innovative properties, nanomaterials including those containing metal nanoparticles may cause certain health risk at all stages of production and product consumption due to their specific physical-chemical properties. They may also be dangerous for human environment objects and lead to grave social and economic consequences.

The challenges that researchers encountered provoked the need to develop reliable methods for characterization of nanoparticles released from various product matrices into complex biological, environmental and food media, and for the assessment of their human and environmental exposure, hazard, and risk [4]. Special attention is paid to detecting correlation between physical properties (i.e., size, shape, surface structure, and aggregation degree) of nanomaterials and toxic response induction in biological structures. This research direction has been actively developed in Federal Scientific Center for Medical and Preventive Health Risk Management Technologies (Perm) for many years. Physical properties of a number of widely spread metal-oxide nanoparticles as well as peculiarities of their biological and toxic effects exerted at various exposure types have not been studied sufficiently; so the research goal is to systemize the knowledge on the subject and to make it more precise.

2. Utilization prospects for nanosized particles of manganese oxide and sources of their introduction into environment

Nanosized particles of manganese oxide (MnO_2) represent a prospective nanomaterial, which can be used for creating high-technology components applicable in nanoelectronics, nano-optics, and nanochemistry [5]. Nowadays, nanodisperse MnO_2 is used as an active component in portable power sources, solar batteries, electrical appliances, accelerators, and sorbents [6, 7]. A possibility to use threadlike nanosized particles of MnO_2 for sensor electrodes creation is of particular interest for researchers [7]. Planned production of matrices based on nanosized MnO_2 for nanomagnetic materials and sorbents, nanoaccelerators, and semiconductor thermistors, can reach up to 1000 tons per year and is considered to be "mass production" [8]. Here, direct exposure of workers involved in the production process, as well as population living in areas influenced by such production, becomes quite possible. A possibility that the substance is introduced into the atmosphere in the form of aerosol is determined by technological processes as nanoparticles of MnO_2 are emitted in their course. Such processes include vacuum-ultrasound laser ablation applied in producing matrices of nanomagnetic materials and sorbents [9]. Laser ablation in suspension of nanodisperse MnO_2 includes local impulse-continuous heating of the substance, sublimation, crystallization, and hydrodynamic processes, which cause formation of nanodisperse MnO_2 aerosol.

Formation of nanodisperse MnO_2 aerosol occurs in production of sensory electrodes, biosensors, [6], cathode accelerators, and semiconductor thermistors [7], when electrochemical deposition is applied; this process means covering graphite rods with stable hydrosol of disperse MnO_2 nanoparticles in electroplating baths. Sewage formed in the processes contains MnO_2, and they can get into surface wells. Today, aerosol of nanodisperse MnO_2 can be found in civil engineering and chemical production facilities. Working area air at a production facility manufacturing potash fertilizers was examined; the research results proved that MnO_2 particles were present in the air; thus, there were about 4435–7330 million/m^3 particles sized 45–95 nm at a carrier driver workplace in a milling workshop (MnO_2 content in working area air was equal to 0.3 mg/m^3). Nanoparticles sized 5–25 nm in concentrations equal to 4588–11,423 million/m^3 were registered at a machine operator workplace in a granulating workshop. Manganese particles were identified among those nanoparticles via mass-spectrometry technique with inductive-bound plasma; Agilent 7500cx mass-spectrometer with octopole reaction collision cell was applied (Agilent Technologies Inc., USA) [10]. There are some data implying that MnO_2 particles can be toxic when introduced in various ways, and it requires further examination of this nanomaterial.

Detailed research on nanosized particles toxicity involves a wide range of tasks according to the recommendations set forth by Good laboratory practice (GLP): toxicology evaluation, single dose, repeated dose, toxicokinetics, genotoxicity, reproductive and developmental toxicology, and local toxicity. According to these recommendations, the authors have assessed toxicity of nanosized MnO_2. All the animals before the experiment underwent 14-day quarantine and were placed in standard cages made of polypropylene, two animals in each. Cages were in a ventilated room. Air temperature in the room was constant and equal to 23.0 ± 2.0°C, and air humidity was 60.0 ± 5.0%. The animals received semisynthetic nutrition with food and biological value, which completely satisfied all physiological needs. They also had free access to food and water. All procedures and examinations on animals were performed in full conformity with guide for the care and use of laboratory

animals (ILAR, DELS) [11] and requirements set forth by Ethics Committee of Federal Scientific Center for Medical and Preventive Health Risk Management Technologies.

3. Results and discussion

3.1 Physical and chemical properties of nanodisperse magnesium oxide

The following substances were tested during the experiment: water suspension of nanodisperse magnesium oxide (III, IV) (manganese (III, IV) oxide, CAS Registry Number 1313-13-09). IUPAC name: manganese oxide and manganese (III, IV) oxide. Synonyms: manganese dioxide, manganese binoxide, and manganese peroxide [12].

According to the results of studying the particle size and shape with independent methods, it is found that the MnO_2 sample tested was a nanomaterial. This is evidenced by the study results of the water suspension test sample (MnO_2 concentration is 36.0 ± 2.3 mg/cm^3) with a residual CTAB in the suspension below the detection threshold (0.00001 mg/cm^3). The particle size distribution (cross-sectional dimension determined with dynamic laser light scattering) is represented in the bar chart as follows: 13 nm (1.2% of the total number of particles), 15–29 nm (94.4% of the total number of particles), and 33–100 nm (4.1% of the total number of particles). The maximum peak value of the particle size made 19 ± 4 nm (41.2% of the total number of particles) (**Table 1**).

Scanning electron microscopy revealed that the particles being visualized exceeded 20 nm in size. The difference with the previous method may be due to a failed focus of the scanning microscope on the nanoparticles smaller than 20 nm, despite sensitivity of 3–10 nm, as stated in its data sheet. As seen in particles are of filamentary shape (97.8% of the total number of particles). The determined sizes and the shape of particles are confirmed by atomic force microscopy (**Figures 1** and **2**).

The textural characteristics of resulting material studied showed that the adsorption-desorption isotherm of nitrogen corresponds to the type IV (isotherm with a distinct capillary condensation), and the shape of the hysteresis loop belongs to H3 type with the distinct area of mesopores filling within the range of relative pressures (p/p_0) 0.7–1. In other words, mesopores filling at higher relative pressures verifies the presence of large diameter mesopores (**Figure 3**).

The maximum pore size distribution occurs in the range of ~10 nm. The specific surface area (S_{BET}) of the nanosized particles, calculated by Brunauer et al. [13], amounted to 150.2 ± 2.6 m^2/g. The total pore volume was equal to 0.676 cm^3/g (the total pores volume (V_{tot}) was calculated from the amount of nitrogen adsorbed at a relative pressure p/p0 ≈ 0.99. Pore size distribution was determined by the desorption isotherms by Barrett et al. [14]).

The water suspension of nanodisperse magnesium oxide had the following physicochemical characteristics: chemical formula: MnO_2, smiles: O═Mn═O, molar mass: 6.9368 g/mol, chemical composition of the nanosized phase: metal, presence of solvent: matrix-bidistilled water, particle charge: neutral at pH = 7.4, resistance to aggregation: particles are prone to aggregation, hydrophobicity: hydrophilic substance, Bp at 76 mm Hg: 3127°C, Bm: 1080°C; vapor tension (mm Hg) and volatility (mg/m^3 20°C): undetermined, specific weight: 4.8 g/cm^3, water solubility: insoluble, oil/water ratio: undetermined, and aggregation state: in water at 20 and 35°C—dark brown solid substance, in air at 20 and 35°C—dark brown powder, of high strength and hardness.

Size of particles in a suspension, micron	Proportion of particles, %
0.0131	1.2
0.0150	9.6
0.0171	16.4
0.0196	20.0
0.0225	21.2
0.0257	13.9
0.0295	13.2
0.0338	0.44
0.0387	0.38
0.0443	0.64
0.0507	0.90
0.0581	0.73
0.0666	0.42
0.0762	0.39
0.0873	0.15

Table 1.
Distribution of MnO_2 nanoparticles in a water suspension versus particle size using dynamic light scattering analyzer Horiba LB-550 (Horiba, Japan) [14].

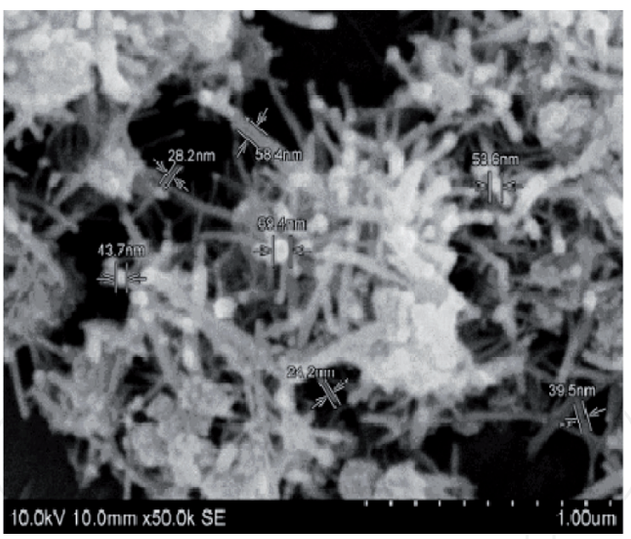

Figure 1.
Scanning electron microscopy image of MnO_2 nanoparticles, electron microscopy with a high-resolution scanning microscope (3–10 nm, max magnification of 300,000X) S-3400 N (Hitachi, Japan) with energy dispersive X-ray attachment for microanalysis (Bruker, Germany) [15].

3.2 Acute toxicity study of nanodisperse manganese oxide at various types of introduction into a body

3.2.1 Acute toxicity study of MnO_2 nanoparticles under inhalation exposure

Over the last decade, a lot of researchers have dedicated their work to practical application of a priority nanomaterial, namely, nanodisperse MnO_2 [16]. They are particularly interested in examining possibilities to use threadlike nanosized MnO_2 particles for sensory electrodes creation [6, 7] or cathode accelerator creation [7] at

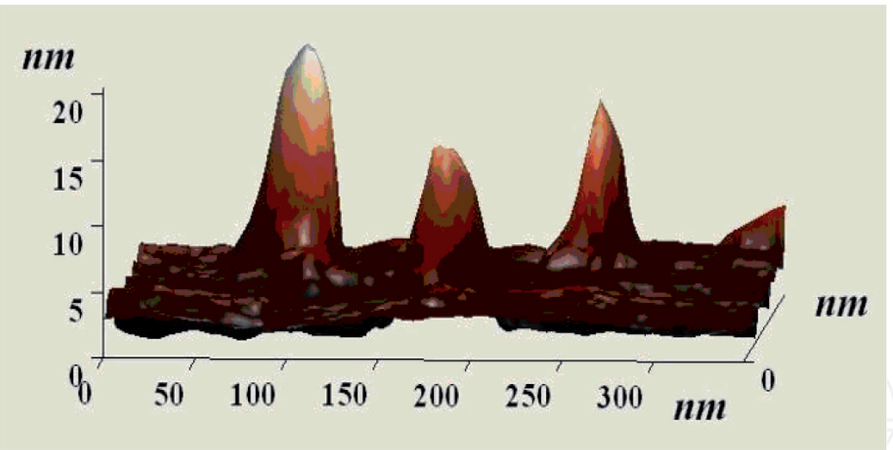

Figure 2.
The 3D-pattern of the MnO_2 nanodisperse particles, atomic force microscopy with the use of solver-PRO microscope (NT-MDT, Russian) [10].

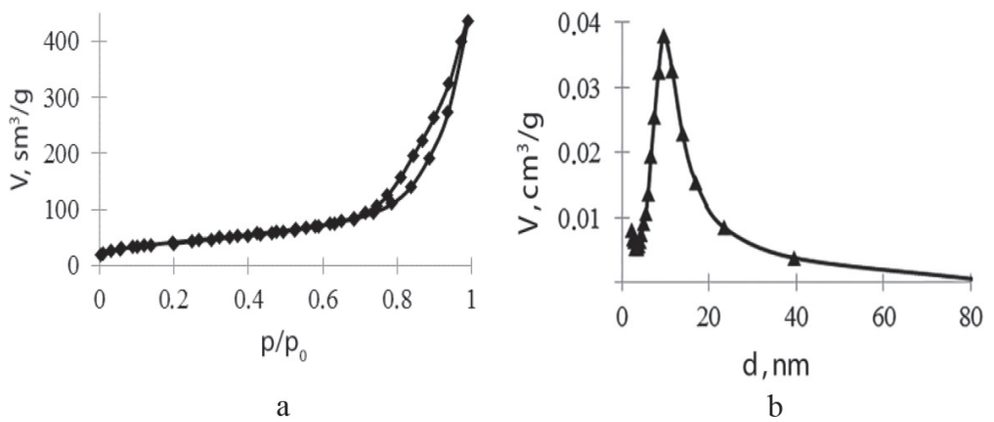

Figure 3.
Nanodisperse MnO_2: (a) nitrogen isotherm adsorption-desorption and (b) pore size distribution d (nm) [15].

covering graphite rods via electrochemical deposition, up-to-date sorbents with the use of vacuum-ultrasound laser ablation [17, 18]. Inhalation exposure of workers to nanosized MnO_2 particles is quite possible during such manufacturing processes as these particles are emitted into working area air. In relation to that, wider utilization of nanosized MnO_2 in industrial production as well as providing workers' safety in the process requires more profound studies on toxicity of nanodisperse MnO_2 when it enters a body being inhaled as an aerosol.

The authors used water suspension of nanodisperse MnO_2 in concentration equal to 36.0 ± 2.3 mg/cm^3 as an examined substance. To make comparison, microdisperse MnO_2 with concentration in manganese water suspension equal to 40.31 ± 1.6 mg/cm^3 was used. The particles size amounted to 5.5–37.0 μm (particles' share 67.0%). The size of microdisperse MnO_2 particles is 194–1300 times greater than the nanodisperse MnO_2 particles size. Specific surface area of MnO_2 nanoparticles (Brunauer-Emmett-Teller technique [13]) was equal to 150.23 m^2/g, which was 1.2 times higher than microparticle-specific surface area (130 m^2/g). This property can cause high MnO_2 nanoparticles reactivity *in vitro* and *in vivo* [19].

To determine acute toxicity parameters, the authors completed an experiment on pubescent Wistar rats (male and female) with body weight equal to 190 ± 10 g. They examined and assessed acute toxicity of nanodisperse MnO_2 water suspension at inhalation introduction as an aerosol in accordance with Interstate Standard "Testing techniques on determining chemical products effects exerted on a human body: acute inhalation toxicity technique determining acute toxicity class

(ATC technique)" (OECD, Test No 436:2008, IDT) (2012). Inhalation introduction into the experimental animals' bodies was modeled in inhalation system with integrated software; and a chamber for a whole body was used in the process (TSE Systems GmbH, Germany). The experimental animals were divided into three groups (experimental groups were 1 and 2, and group 3 was a control one, n = 18 animals). Experimental group 1 was exposed to the examined substance inhalation at substance nominal concentration in the chamber equal to 0.05 mg/l; concentration for experimental group 2 was equal to 0.5 mg/l. The exposure lasted for 4 hours; the animals received no nutrition during the process. After inhalation exposure, the animals were observed during next 96 hours to detect possible delayed substance toxicity. Control group was exposed to inhalation of distilled water in the form of an aerosol under analogous conditions. The water conformed to TU 6-09-2502-77. After observation period for the animals from experimental groups 1 and 2 was over, they were taken out of the experiment via sparing euthanasia. Brains were extracted with a special instrument and fixed in 5% solution of buffered neutral formalin. Fixed tissue pieces were dehydrated in Excelsior ES automatic histological processor (Thermo Scientific, Germany). The finished specimens were examined in Axio Lab A1 light-optical microscope, micropictures were taken with the use of Mikroskopkamera AxioCam ERc 5 s (Carl Zeiss, Germany) at magnification equal to ×400.

The results of all research performed with independent techniques application helped to detect that the examined MnO_2 sample was a nanomaterial. The examination of the tested substance suspension in concentration equal to 36.0 ± 2.3 mg/cm^3 proves it. Particle size distribution on the bar graph is as follows (particles cross-section size is presented): 13 nm (1.2% of the total particles number), 15–29 nm (94.4%), and 33–100 nm (4.1%). Maximum peak of particles size corresponded to 19 ± 4 nm (41.2%). Scanning electron microscopy technique enabled detecting that visualized particles size exceeded 20 nm. Assessment of nanoparticles quantity in the inhalation chamber area showed that when nanodisperse fraction is fed into the chamber and transfers into aerosol, it does not agglomerate to micrometer range (**Figures 4** and **5**). The size of most particles (99% from the total quantity) does not exceed 100 nm at the examined actual concentrations after 2–4 hours of exposure.

Clinical picture of acute intoxication at inhalation exposure to nanodisperse MnO_2 aerosol at actual concentration equal to 0.029 ± 0.001 mg/dm^3 was characterized with evident neurotoxic effects, which started to occur in male and female rats from experimental group 1 after 3 hours of exposure. Animals had movement coordination disorders, took unusual postures, and showed weaker reaction to sound stimulus; all these effects remained in survivor animals during 48 hours after exposure. When actual concentration was equal to 0.472 ± 0.005 mg/dm^3, rats started to suffer from apparent respiratory failure after 30 minutes of exposure.

Most rats in experimental group 2 (three male and two female) died within 150–190 minutes after the experiment started; their death was caused by acute respiratory failure. One female rat died 2 hours after the experiment was over. The animals were sluggish before their death, they took lateral position, and demonstrated no reaction to sound stimulus or motion activity. Death of the experimental animals was not established. CL_{50} of the examined nanodisperse MnO_2 amounted to 0.12 mg/l. This concentration is within 0.05–0.5 mg/l range, which allows to define the tested substance as having the second hazard class "ATC technique" (OECD, Test No. 436:2008, IDT). It is known that minimal toxic concentration (TCL_0) of nanosized MnO_2 for rats at inhalation introduction during 24 hours amounts to 1.8 mg/m^3; for mice during 7 hours, 49 mg/m^3 (data taken from Minimal lethal dose (LDL_0) for rats at intratracheal introduction amount to 45 mg/kg. Safety specification does not contain any additional information regarding errors, confidence limits, or animals sex. Morphologic changes in brain tissues of the rats from

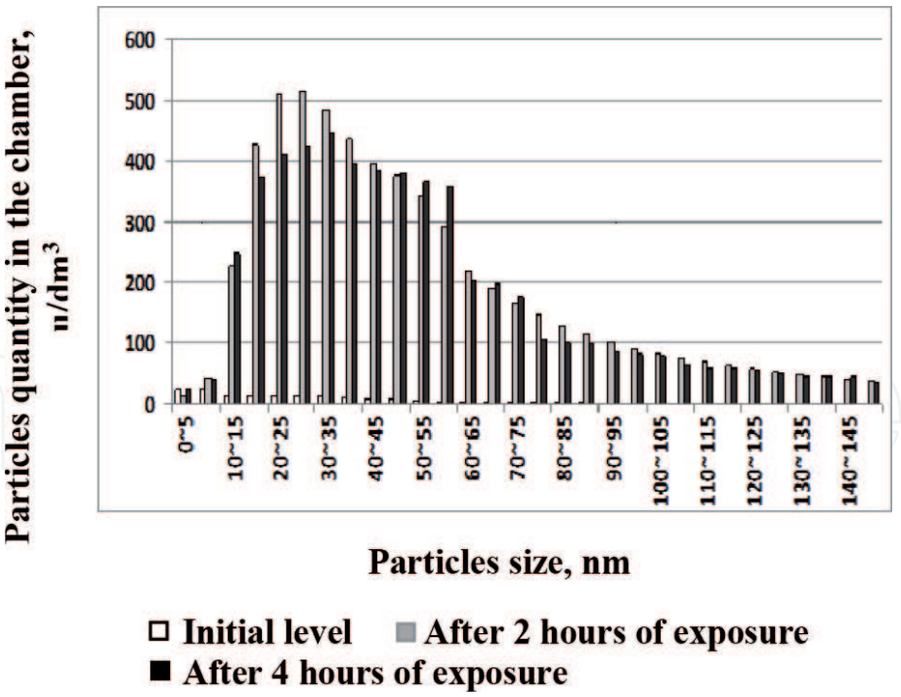

Figure 4.
Nanoparticle concentration in the inhalation chamber air at actual MnO_2 concentration equal to 0.029 ± 0.001 mg/dm³ [15].

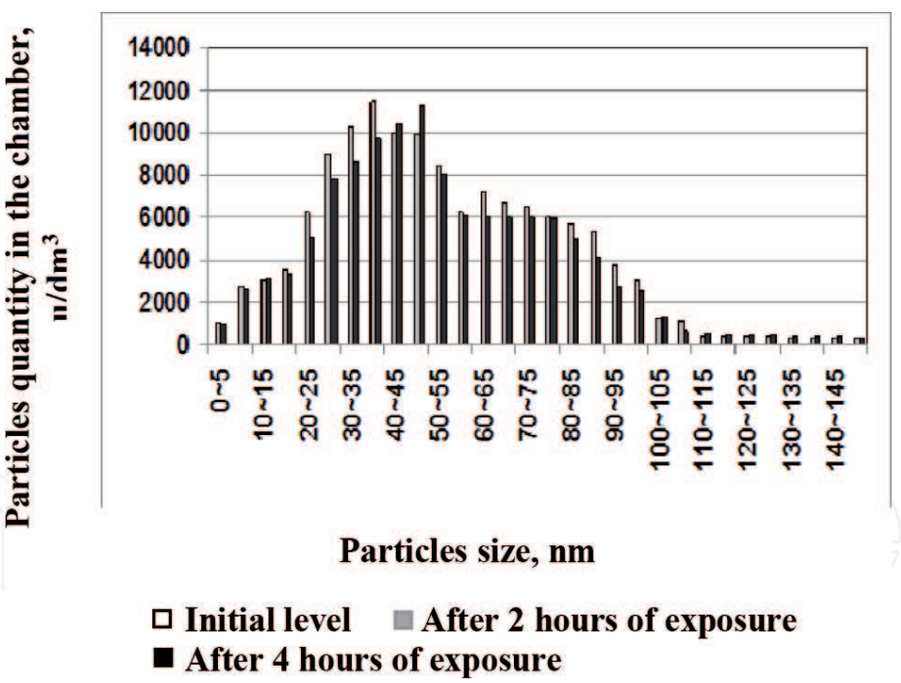

Figure 5.
Nanoparticle concentration in the inhalation chamber air at actual MnO_2 concentration equal to 0.472 ± 0.005 mg/dm³ [15].

experimental group 1 in comparison with control group were characterized with the following pathologic disorders: brain substance vessels were filled with blood insignificantly or moderately and had focal endothelium swelling and perivascular spaces dilatation. The most apparent changes in brain tissue of the rats from experimental group 1 occurred in cerebellum. Neurons and neuroglia cells were characterized with grave ischemic damages in the form of wrinkling and pyknosis. Nerve fibers of brain tissue looked spongy and were unevenly colored, had fizzy contours, and focal prolapse of glial elements (**Figure 6**).

The results obtained in the course of the research indicate that the examined nanosized MnO_2 particles can cause neurotoxic effect and respiratory failure; the combination of these two factors could lead to the animals' death. The obtained results are confirmed by research performed by a number of authors [20, 21], which prove that MnO_2 nanoparticles exert toxic effects at inhalation exposure. Thus, after 24-hour exposure, catalytic generation of active oxygen forms (AOF) in human alveolar epithelial cells [20] increased; level of extracellular and intracellular oxidized glutathione form (GSSG) also grew by 30 and 80% correspondingly [20, 21]. Manganese oxide (IV) nanoparticles sized up to 30 nm are able to penetrate into neuron-like PC-12 cells of a brain at inhalation exposure via olfactory nerve [22] and accumulate in astrocytes [17, 23].

Here, slight mitochondrial activity inhibition occurs; dose-dependent decrease in dopamine and its metabolites (3,4-dihydroxyphenylacetic acid and homovanillic acid) takes place. This process is accompanied with a multiple AOF growth [20, 24] and becomes apparent in experimental animals through neurodegenerating disorders as early as after 2 or 3 weeks of exposure [20, 23, 24]. It is proved that MnO_2 nanoparticles (III, IV) can accumulate in brain cells [25, 26]. In particular, astrocytes are able to accumulate MnO_2 nanoparticles and produce AOF [25, 27, 28]. This process is accompanied with protein cleavage activation mediated by caspase-3 and protein kinase Cδ (these are enzymes that participate in apoptosis, necrosis, and inflammatory processes), as well as phosphorylation cycle activation [25, 26]. As particles concentration increases, level of p38 mutagen-active protein kinase grows linearly; this protein kinase activates apoptotic mechanism of untimely cell death [24, 29–31]. Tumor necrosis factor-α doubles in olfactory bulb, frontal cortex, midbrain, and striate body [27]. If inhalation exposure to MnO_2 nanoparticles (III, IV) is long-term, time-depending activation of transferrin in dopaminergic nervous cells is detected, as well as structural changes in Beclin 1 and LC3 proteins, which, in its turn, can be an evidence of potential autophagia process activation [20].

As per data taken from the annotated scientific literature, it is proved that toxic effects exerted on nervous system cells can be caused both by nanoparticles [25, 29] and by microdisperse analog at a low-dose exposure [32]. Disorders in neurons membranes functions can underlie the neurotoxic action mechanism; such disorders result from membranes lipid peroxidation which in its turn is caused by direct cytotoxic effect of nanoparticles determined for dopaminergic

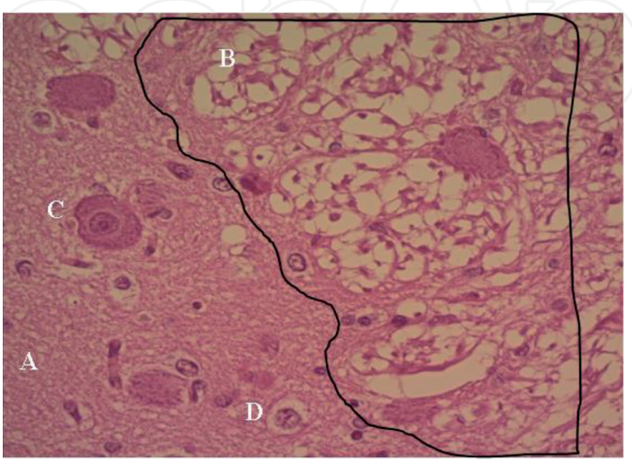

Figure 6.
Cerebellum of a Wistar rat after acute inhalation exposure to nanodisperse MnO_2 aerosol at actual MnO_2 concentration in the inhalation chamber area equal to 0.029 ± 0.001 mg/dm³ (painted with hematoxylin-eosin, ×400): A is cerebellum tissue without changes, green; B is ischemia focus (grave ischemic changes), edema (damage zone is outlined); C is motor neuron of cerebellum subcortex; and D is glia cells with pericellular space dilatation [15].

neurons [25, 29, 33]. This effect can be more apparent for nanodisperse particles in comparison with microdisperse analog effects due to the fact that nanoparticles have a greater specific surface area.

Mechanism of nanodisperse MnO_2 neurotoxicity is related to the ability to generate free radicals and to interact with proteins. Manganese oxide nanoparticles are able to actively generate free radicals when they interact with bilipid layer of cell membranes [25, 30]. When interacting with cell membranes, they stimulate excessive creation of active oxygen forms (AOF), which is accompanied with high catalytic activity and cell apoptosis [25, 26, 30]. Oxidized (GSSG) and reduced glutathione form (GSH) content is one of the parameters showing oxidative stress level. It is proved that if alveolar epithelial cells are exposed to MnO_2 particles for 24 hours, the level of extracellular and intracellular GSSG increases by 30 and 80% correspondingly; at the same time, caspase-3 activity grows and this enzyme is known to induce apoptosis processes. GSH concentration increases after 24-hour exposure to the examined substance, and it can be caused by activation of γ-glutamylcysteine synthetase synthesis and more active feed system of cystine and glutamate amino acids, which are substrates for synthesis of reduced glutathione form [25]. A significant increase in GSSG in a cell induced by MnO_2 nanoparticles can be caused by manganese particles entering reduction reaction with superoxide formation, which, under superoxide dismutase effects, is converted into oxygen and hydrogen peroxide. Then, hydrogen peroxide decomposes with the help of reduced glutathione form, and it leads to GSSG increase. Another possible way of hydrogen peroxide transformation in a cell is hydroxyl radicals creation in the presence of manganese ions; these radicals are also able to oxidize GSH with creation of GSSG [26].

Clinical picture of acute intoxication, detailed in the previous works by the authors [34], confirms the mechanism of toxic effects exerted by nanodisperse MnO_2 particles which a number of authors describe in above-mentioned scientific works [27, 28]. Respiratory failure evolvement can also be related to potential ability of the examined nanoparticles to cause inflammatory changes with consequent apoptosis of alveolar epithelial cells. At the same time, MnO_2 nanoparticles have greater resistance to mucociliary clearance; therefore, they are in a longer contact with respiratory tract cells in comparison with microdisperse analog [28].

3.2.2 Examination of acute toxicity which nanodisperse MnO_2 has at oral introduction

Intensive development of the major promising nanotechnological spheres such as nano-optics, nanoelectronics, pharmacology, chemistry, and metallurgy has direct influence on growth of nanodisperse MnO_2 production volumes. Nanosized MnO_2 particles are widely used in production of matrixes for nanomagnetic materials and sorbents [35], nanoaccelerators, semiconductor thermistors [36]. Wastes of such productions can get into sewage and then into water reservoirs serving as sources for drinking water supply. MnO_2 nanoparticles are known to have nonspherical form, which makes for lower speed of their excretion out of a body with the help of immune system's phagocytes through lymphatic ducts and causes their longer contacts with body tissues [19]. In relation to that it is reasonable to think that profound examination of nanodisperse MnO_2 aerosol toxicity at oral introduction with water into a body is of great importance for securing production workers safety and safety of population living in areas influenced by such productions.

The authors examined nanodisperse MnO_2 water suspension with particles sized 15–29 nm. Particles were thread-like and had surface area equal to 150.2 ± 2.6 m^2/g. MnO_2 concentration in nanodisperse solution was equal to 36.0 ± 2.3 mg/cm^3.

The detailed description of synthesis and physical and chemical properties of nanodisperse MnO_2 is given in the precious works [37, 38]. To make comparison, microdisperse MnO_2 with concentration in manganese water suspension equal to 40.31 ± 1.6 mg/cm^3 was used. The particle size amounted to 5.5–37.0 μm (particles' share 67.0%) (dynamic light scattering technique with the use of Microtrac S3500 laser analyzer (Microtrac, the USA)). The size of microdisperse MnO_2 particles is 194–1300 times greater than nanodisperse MnO_2 particle size. Specific surface area of MnO_2 nanoparticles (Brunauer–Emmett–Teller technique [13]) was equal to 150.23 m^2/g, which was 1.2 times higher than microparticles specific surface area (130 m^2/g). Acute toxicity parameters of nanodisperse MnO_2 were assessed as per the results of comprehensive acute experiments performed in accordance with methodical guidelines [10] on nonlinear male white mice with body weight equal to 27 ± 2 r (M ± m) (n = 70); the animals belonged to a conventional category. Nanodisperse MnO_2 was introduced into mice's bodies a single time via gastric tube in various doses: group 1 received 2000 mg/kg of body weight, group 2–3500 mg/kg, and group 3–5000 mg/kg. The tested sample was introduced in a form of water suspension in volume equal to 1–2% of the animals' body weight. Microdisperse MnO_2 was introduced into mice from experimental groups 4, 5, and 6 in the same doses as in groups 1, 2, and 3. The tested samples were introduced in the same way. Control group 7 received water a single time via gastric tube in the same volume. The observation term after the tested substances was introduced amounted to 14 days. Mice were kept in cages: five animals in each.

The experiment revealed that clinical picture of acute intoxication at introducing nano- and microdisperse MnO_2 solutions is uniform and nonspecific. Animals from experimental groups 1–6 suffered from hyperexcitability and convulsions during the first 20 minutes of the experiment; then inhibition state occurred, animals' reaction to sound and pain became weak, they had hypopnoe. Animals in experimental groups 2 and 3 died mostly during the first 24 hours; in group 1, during 48 hours; and in comparison groups 5 and 6 in the period from 48 to 72 hours. No mice from group 4 or 7 died in the course of the experiment. It was detected that if nanodisperse MnO_2 solution was once introduced into a body via gastric tube, LD_{50} amounted to 2340 ± 602.6 mg/kg of body weight (third hazard class); in case of microdisperse MnO_2 solution introduction, the dose was equal to 6000 ± 485.6 mg/kg (fourth hazard class). Average death time (TL_{50}) for mice after intragastric introduction of nanodisperse MnO_2 solution amounted to 35.2 hours. When microdisperse MnO_2 solution was introduced, TL_{50} amounted to 32 hours. Cumulation index amounted to 0.79 for nanodisperse MnO_2 particles. If cumulation index is >5, one can assume that nanoparticles are hypercumulative. Cumulation index is equal to 0 for microdisperse MnO_2 particles. If cumulation index is equal to 0, one can assume that particles are moderately cumulative [39].

Analysis of changes, which occurred in venous blood of the experimental animals, revealed that nanoparticles of disperse MnO_2 solution in a dose equal to 3500 and 5000 mg/kg exert more apparent toxic effects on erythrocytes and thrombocytes in comparison with a microdisperse analog. It is confirmed by polychromatocytes occurrence as their share amounted to 20 and 35% of the total erythrocytes number in peripheral blood of mice from experimental groups 2 and 3 correspondingly. When microdisperse MnO_2 was introduced in the same doses polychromatocytes share in mice's blood amounted to 10 and 15% correspondingly. 10–20% of erythrocytes in blood of mice from those groups contained pathologic Jolly bodies and it was two times higher than the same parameter in blood of mice from experimental groups 5 and 6 correspondingly. Nanodisperse MnO_2 solution caused massive thrombocytes aggregation in blood of mice from experimental groups 2 and 3. Microdisperse MnO_2 solution when introduced into mice in a dose

equal to 5000 mg/kg (experimental group 6) led to only sporadic occurrence of thrombocytes aggregation. There were no pathologic changes in blood slides of mice from experimental group 7.

Morphological examinations after introducing nanodisperse MnO_2 solution in a dose equal to 3500 mg/kg revealed changes in all examined organs taken out of mice. There was significant dilatation and hyperemia of veins in liver and kidneys, considerable blood overflow in veins of cardiac muscle and epicardium, as well as in heart chambers. There were hemorrhages detected in medullar substance of kidneys. Proliferative processes occurred in macrophage and lymphoid systems of experimental animals. An increased number of macrophages and their activation was detected in liver, in both kidneys and, in particular, in lungs (**Figure 7**). Kupffer cells in liver are enlarged and bulged into sinusoid capillaries lumen; mesangial cells in renal bodies are hypertrophic, and numerous alveolar macrophages contain phagocyte material. Lymphoid nodules in spleen white pulp are enlarged, tend to fuse, and there is no typical division into zones in them. Red pulp prevails in the organ together with diffuse and focal lymphatization occurrence. Proliferation of cells from lymphocytes and macrophages range leads to leukocytic infiltration of parenchymatous organs. Numerous periportal and intralobular lymphoid-histiocytic infiltrates occur in liver; perivascular and intertubular ones are observed in kidneys. Organ infiltration with lymphocytes is so active that it can penetrate through blood-brain barrier; lymphoid infiltrates can be detected even in white substance of cerebral hemispheres (**Figures 8–10**).

When a microdisperse MnO_2 solution in a dose equal to 3500 mg/kg was introduced, it led to some dilatation of sinusoid capillaries in liver and vessels of renal microcirculatory bed. Capsule lumen in some renal corpuscles was dilated. Occasional lymph-histiocytic infiltration occurred in parenchymatous organs. Infiltrates were located only in connective tissue and were rather small. As opposed to group 2, animals from group 5 had no infiltrates in brain hemispheres cortex. There was only slight perivascular and moderate pericellular edema located mostly in granular layer.

Therefore, mice from group 2 after a single introduction of nanodisperse MnO_2 solution in a dose equal to 3500 mg/kg via gastric tube had more apparent morphological changes in internal organs than mice from group 5 (microdisperse analog). These changes were detected in circulatory system and characterized with dilatation and hyperemia of veins in all the studied organs. Blood overflow in veins of cardiac

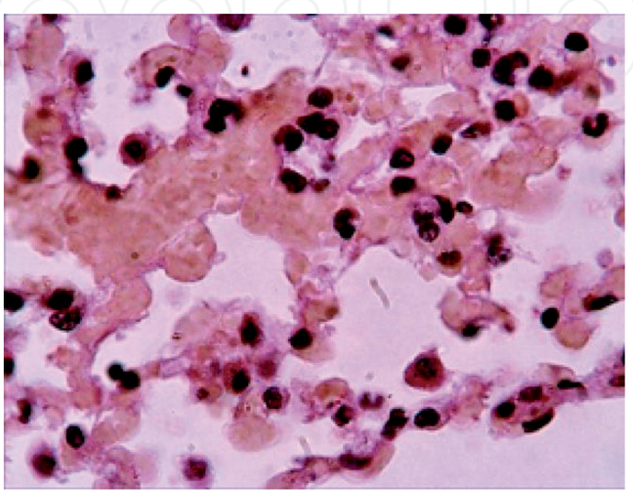

Figure 7.
Macrophage reaction in a lung of a mouse from experimental group 2, which died during the first day after nanodisperse MnO_2 in a dose equal to 3500 mg/kg, was introduced. The specimen was painted with hematoxylin and eosin, and the magnification was equal to ×1000 [38].

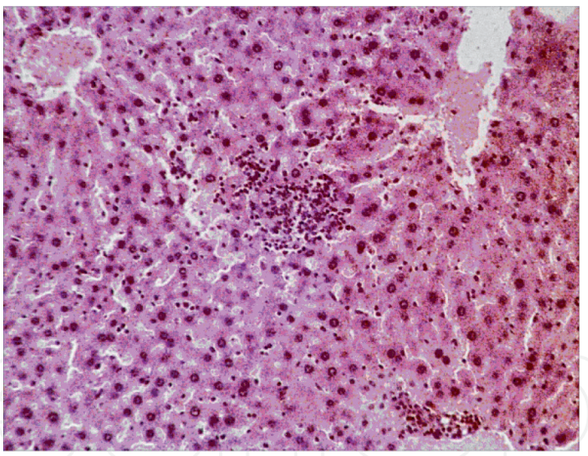

Figure 8.
A nonlinear mouse from experimental group 2, which died during the first day after nanodisperse MnO_2 in a dose equal to 3500 mg/kg, was introduced. Lymph-histiocytic intralobular infiltrates in a liver. The specimen is painted with hematoxylin and eosin, and magnification is equal to ×200 [38].

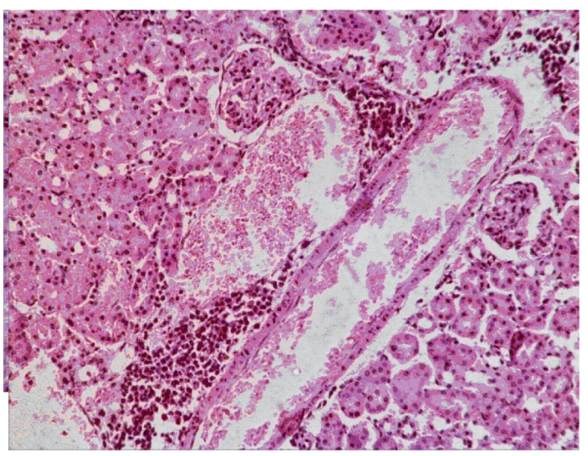

Figure 9.
A nonlinear mouse from experimental group 2, which died during the first day after nanodisperse MnO_2 in a dose equal to 3500 mg/kg, was introduced. Lymph-histiocytic perivascular infiltrates in a kidney. The specimen is painted with hematoxylin and eosin, and magnification is equal to ×200 [38].

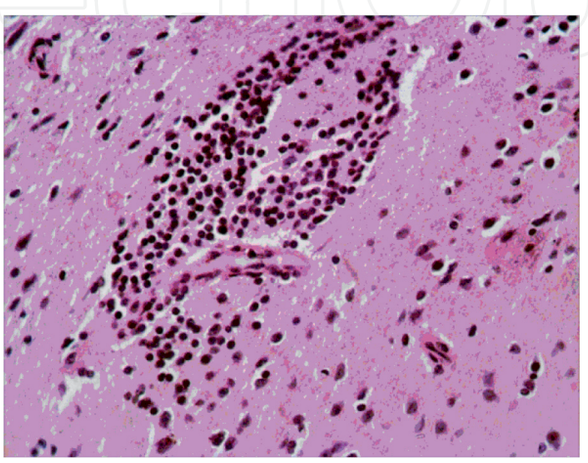

Figure 10.
A nonlinear mouse from experimental group 2, which died during the first day after nanodisperse MnO_2 in a dose equal to 3500 mg/kg, was introduced. The specimen is painted with hematoxylin and eosin, and magnification is equal to ×400. Lymphocytic infiltration in white substance of cerebral hemispheres [38].

muscle, epicardium and all heart chambers was particularly evident. Mice from group 5 had no peculiar morphological changes in circulatory system organs. Mice from group 2 had proliferative processes in lymphoid and macrophage systems. These processes were morphologically apparent through hypertrophy of thymus lobules cortex, lymphoid follicles of spleen white pulp and lymphatization of spleen red pulp, and macrophage activation in liver, kidneys and lungs. Such morphological changes did not occur in mice from group 5. Proliferation of lymphoid cells and macrophages leads to histioleukocytic infiltration of parenchymatous organs. And here, processes caused by nanodisperse MnO_2 solution impact are more apparent than those caused by microdisperse MnO_2 solution. Morphological changes are determined by vascular disorders in venous bed, which result in hemorrhages in parenchymatous organs, especially in kidneys. There were none of such morphological changes in mice when microdisperse MnO_2 solution was introduced into them. The analysis of the obtained results allows to make a conclusion that nanodisperse MnO_2 solution at a single introduction via gastric tube has LD_{50} equal to 2340 ± 602.6 mg/kg (third hazard class), which is 2.6 times higher than LD_{50} equal to 6000 ± 485.6 mg/kg at a single introduction of microdisperse MnO_2 solution (fourth hazard class). Nanodisperse MnO_2 solution at single introduction into mice via gastric tube in a dose equal to 3500 mg/kg exerts hemotoxic effects, which reveal themselves in a form of pathologic inclusions in erythrocytes and increased thrombocytes aggregation. There were also certain circulation disorders observed such as vein dilatation and hyperemia, as well as filling of their lumen with erythrocytes, which leads to hemorrhages in all the studied organs. Proliferative processes in lymphoid and macrophage systems were detected; they result in hypertrophy of thymus lobule cortex and lymphoid follicles of spleen white pulp, lymphatization of spleen red pulp, and macrophages activation in liver, kidneys and lungs.

3.3 Studying subchronic and chronic toxicity of nanodisperse manganese oxide water suspension at intragastric introduction via gastric tube

Studying subchronic toxicity of nanodisperse MnO_2 water suspension at intragastric introduction via gastric tube: nowadays, there is a growing interest in using MnO_2 nanoparticles as a sorbent and catalyst for complex purification of liquid radioactive wastes, which are dangerous for human health. But MnO_2 nanoparticles can get into sewage in the process and later they can be found in surface water reservoirs used for drinking water supply to population. In relation to that, study of toxic effects exerted by MnO_2 nanoparticles at oral introduction with drinking water matters a lot if one wants to assess their safety.

Experimental research dedicated to nanodisperse MnO_2 were performed with intragastric introduction via gastric tube during 90 days. During this particular research, nanodisperse MnO_2 water suspension was introduced into Wistar rats (males and females) with body weight equal to 200 ± 10 g (n = 100) via gastric tube daily for 90 days. Animals were divided into four experimental groups and 1 control group, 20 animals in each. Nanodisperse MnO_2 water suspension was introduced in the following doses: group 1—257.7 mg/kg (1/10 LD_{50}), group 2—51.54 mg/kg (1/50 LD_{50}), group 3—10.3 mg/kg (1/250 LD_{50}[3]), group 4—5.15 mg/kg (1/500 LD_{50}), and group 5 (control one)—distilled water in volume equal. Nanodisperse MnO_2 water suspension dispersion was accomplished directly before carrying out the research and later on a weekly basis during 90 days, while the experiment was lasting in order to achieve even particles distribution in a volume of liquid; the procedure was done with the use of ultrasound at room temperature under continuous pulsation at 65%-power for 2 minutes. The following parameters were assessed: body weight dynamics, as well as changes in biochemical parameters of neurons functions and

oxidation-antioxidant system balance. Morphological changes in brain tissues were studied via histological specimens microscopy (magnification ×400).

Body weight dynamics analysis performed on rats from group 1 revealed authentic decrease in this parameter by 7.7% by the 30th day of the experiment in comparison with the baseline. Body weight was recovered by the 90th day. Decrease in body weight of rats from group 1 authentically differed from this parameter in control group during the whole experiment. In all other groups, authentic increase in body weight of experimental animals was detected. Examination and assessment of biochemical parameters characterizing neurotransmitters balance and oxidation-antioxidant system at long-term introduction of nanodisperse MnO_2 water suspension proves negative effects occurrence; these effects are dose depending. There was an authentic increase in lipid hydroperoxide level in blood serum of rats on the 30th day of the experiment when doses were 10.0–260 mg/kg of body weight; this parameter was 1.4–1.9 times higher than the baseline in rats from the control group ($p < 0.001$). Malonic dialdehyde level in blood serum of rats was 1.6–2.0 times higher than the baseline of this parameter in control group rats, the doses being equal ($p < 0.001$). On the 90th day, high levels of lipids hydroperoxides and malonic dialdehyde in blood serum remained. The order of discrepancy between the baseline and parameters in the control group was 1.3–1.9 times ($p < 0.001$). When a dose was equal to 5.0 mg/kg, there were not any authentic discrepancies between these parameters and the baseline, or between them and control group parameters during the whole experiment. When doses were 10.0–260 mg/kg, an authentic decrease in Cu/Zn-SOD and OAS in blood serum of rats was registered; this decrease was dose dependent. During the whole experiment, Cu/Zn-SOD level was on average from 1.4 to 4.6 times lower than the baseline and the control group parameter ($p < 0.001$–0.002). OAS level was 1.6–5.4 times lower ($p < 0.001$). When a dose was equal to 5.0 mg/kg, there were no authentic discrepancies in OAS level between experimental and control group during the whole experiment.

Assessment of basic neurotransmitters content in blood serum of rats on the 90th day of the experiment revealed authentic increase in glutamate level and decrease in GABA level in comparison with the baseline and control group. Changes in these parameters were dose dependent. Glutamate level in blood serum grew from 2 to 3.8 times depending on a dose ($p < 0.001$). GABA level in blood serum decreased 2.3–2.7 times ($p < 0.001$). When a dose was equal to 5.0 mg/kg, there was no authentic decrease in the analyzed parameters in blood serum against control group parameters. The obtained results show that, given their small size and high penetrability, MnO_2 nanoparticles can penetrate through blood-brain barrier and cause morphological-functional disorders in various sections of central nervous system when introduced into a body in different ways even in relatively small concentrations [27].

The detected activation of cell membranes lipid peroxidation and imbalance in CNS neuromediators at intragastric introduction of nanodispersed MnO_2, in Wistar rats, are confirmed by the results obtained by a number of authors at other ways of introduction into a body (for example, at intranasal, intratracheal, and inhalation introduction). As a number of authors state, when MnO_2 particle dose equals to 2.63 mg/kg and intranasal introduction of this dose lasts for 6 weeks, neurotoxicity can be observed as relative refractory period of a tail nerve grows [27]. Intratracheal introduction of MnO_2 nanoparticles in a dose equal to 2.63 mg/kg during 6 weeks leads to significant decrease in body weight, longer absolute refractory period of a tail nerve, and lower animals movability [27]. Neurotoxicity of MnO_2 nanoparticles at intratracheal introduction in doses equal to 2.63 and 5.26 mg/kg can be seen through increase in latent period of cortical potential occurrence (total response of large cortex neurons populations to synchronous impulses flow coming to them

and caused by afferent irritator) in visual, auditory, and the first somatosensory area. This effect can be determined by disorders in neuron membranes functions as a result of membrane lipid peroxidation accompanied with calcium homeostasis disorders [23]. Nanoparticles and microparticles of MnO_2 in concentration equal to 100 μg/kg in saline were injected into rats once a 2 weeks during 14 weeks, and it allowed to determine that both substances caused authentic increase in dextrose and cholesterol level. MnO_2 nanoparticles lowered the level of high-density lipoproteins at the sixth, twelfth, and fourteenth week, while microdisperse analog caused such decrease at the twelfth week only. Researchers detected no authentic changes in triglyceride concentration. Changes in biochemical profile might be caused by oxidizing possibilities, which MnO_2 nanoparticles have [40]. An injection of MnO_2 nanoparticles into a rat's brain (in substantia nigra and tegmentum ventral area) in concentration equal to 87 μg/μl in 1 μl causes changes in locomotor abilities and spatial memory, which are related to dopaminergic neuron disorders and inflammation caused by nanoparticles. MnO_2 nanoparticles lead to early symptoms of extrapyramidal disorders with selective loss of dopaminergic neurons [27].

Histological specimens made of experimental animals' brains were assessed; the assessment results allowed to detect morphologic changes in tissue structure depending on a dose of nanodisperse MnO_2 water suspension. After a dose equal to 260 mg/kg of body weight a day had been introduced, the authors detected substantial vessels hyperemia in brain hemispheres cortex and cerebellum together with erythrocytes diapedesis and formation of subarachnoid hemorrhages focuses. There was also brain edema with perivascular and pericellular spaces dilatation (**Figure 11**). Focuses of nerve fibers demyelinization were detected as white substance fibers were unevenly painted and lighter areas with fizzy contours occurred.

After a 50 mg/kg dose focal perivascular and pericellular spaces dilatations form in brain cortex layers, but cortex layers still remain differentiated (**Figure 12**). Vessels in brain cortex tissues substance have thin walls, are moderately filled with blood, the endothelium is flattened, and there are small focal subarachnoid hemorrhages and focal neurons dystrophy zones. A slight perivascular spaces dilatation occurred after a 10 mg/kg of body weight a day (**Figure 13**). But when a dose was equal to 5 mg/kg of body weight a day, morphologic picture of brain and cerebellum tissues corresponded to that of control group; structure patterns were preserved in all the sections (**Figure 14**).

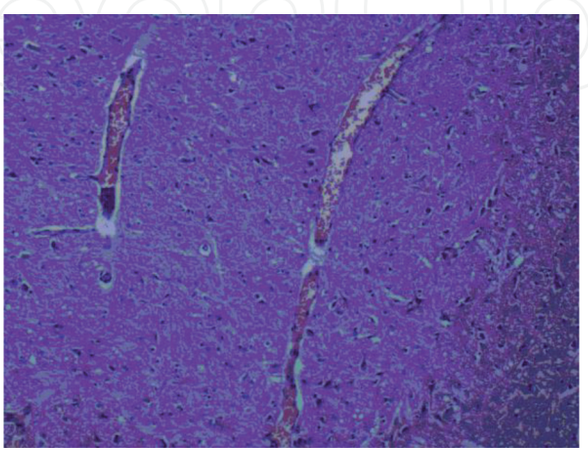

Figure 11.
Brain hemispheres cortex of a rat at intragastric introduction of nanodisperse MnO_2 water suspension in a dose equal to 260 mg/kg of body weight a day, 90th day of the experiment. There are dilated perivascular and pericellular spaces in brain cortex layers. Painted with hematoxylin and eosin, magnification ×400 [41].

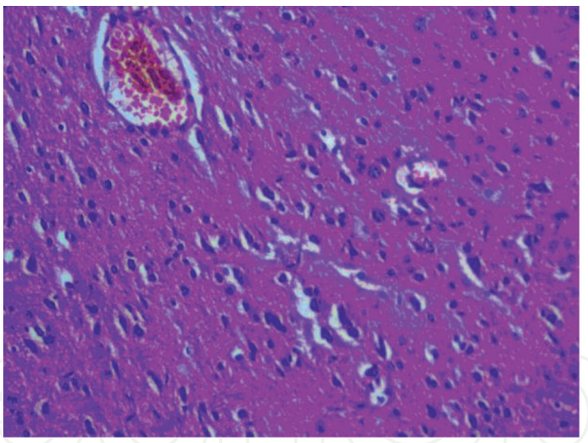

Figure 12.
Brain hemispheres cortex of a rat at intragastric introduction of nanodisperse MnO_2 water suspension in a dose equal to 50 mg/kg of body weight a day, 90th day of the experiment. There are dilated perivascular and pericellular spaces in brain cortex layers. Painted with hematoxylin and eosin, magnification ×400 [41].

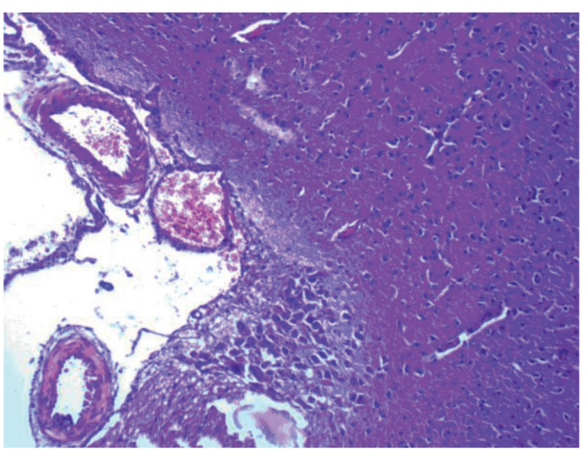

Figure 13.
Brain hemispheres cortex of a rat at intragastric introduction of nanodisperse MnO_2 water suspension in a dose equal to 10 mg/kg of body weight a day, 90th day of the experiment. There is slight perivascular spaces dilatation in brain hemispheres cortex. painted with hematoxylin and eosin, magnification ×100 [41].

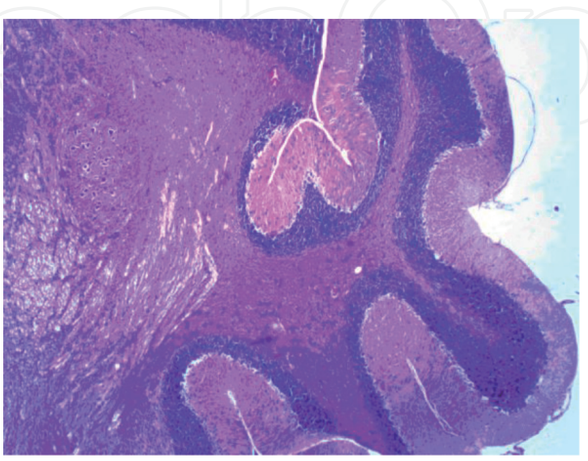

Figure 14.
Cerebellum of a rat at intragastric introduction of nanodisperse MnO_2 water suspension in a dose equal to 5 mg/kg of body weight a day, 90th day of the experiment. Tissue structure pattern in all cerebellum sections is preserved and corresponds to that of control group. Painted with hematoxylin and eosin, magnification ×100 [41].

Brain cortex tissues layers are differentiated quite well. External granular layer is formed out of solid bunch consisting of numerous small neurons; pyramidal layer of brain cortex is wide and consists of polymorphous neurons. Internal granular layer of brain cortex and cerebellum is thin, noncontinuous, made of small pyramidal and stellate cells; ganglionic layer cells in brain cortex tissues are large, polymorphous with dark nucleuses, diffusely located; there is a great number of diverse neurons (they differ in form and size) in polymorphous cells layer. Ganglionic layer in cerebellum tissue has one raw of Purkinje cells with well-developed eosinophilic granular cytoplasm and rounded dark nucleuses. Molecular layer in cerebellum tissue is spongy and contains a small number of minor cells. White substance in brain and cerebellum tissue is made of evenly painted nerve fibers bunches and rounded glia cells. Brain vessels have thin walls and are feebly or moderately filled with blood.

Comparison of pathomorphologic effects occurring at intragastric introduction of nanodisperse MnO_2 water suspension and microdisperse MnO_2 water suspension in a dose equal to 10 mg/kg during 90 days showed that pathomorphologic changes in brain and cerebellum tissues were much more apparent and wide-spread when nanodisperse MnO_2 was introduced. After introduction of nanodisperse MnO_2 water suspension more apparent changes occurred in circulatory system in a form of hemodynamic disorders with focal feeble and moderate vessels hyperemia in brain, liver, lungs, kidneys, and heart; there were also subarachnoid hemorrhages in brain. Changes in lymphatic system became evident through feeble and moderate perivascular lymph-macrophage infiltrates in lungs tissue penetrating into adjacent alveoli. Pathologic changes in macrophage system were apparent through alveolar macrophages activation with formation of small bunches in alveoli lumen. After introduction of microdisperse MnO_2 water suspension changes are represented by focal vessels hyperemia, subarachnoid hemorrhages in brain, small focal lymph-microphage infiltrates in lungs and gastrointestinal tract. Besides, after introduction of nanodisperse MnO_2 water suspension there was perivascular and pericellular spaces dilatation in brains, feebly apparent perivascular thin fibrous cardiosclerosis and feebly apparent focal protein dystrophy in hepatocytes; no such effects were detected after microdisperse MnO_2 introduction.

All the obtained materials were summarized; it allowed to make an assumption on a possible mechanism of toxic impact exerted by nanodisperse MnO_2 particles at oral introduction. Lipid peroxidation activation caused by direct damaging impact exerted by nanodisperse MnO_2 particles on bilipid layer of cytoplasmatic membrane can underlie the whole process [42]. High levels of lipid hydroperoxides and malonic dialdehyde in blood serum are the evidence of this effect. Lower levels of Cu/Zn-SOD and OAS in blood serum prove antioxidation processes insufficiency. The results obtained in the research showed that astrocytes and neurons membranes are the first targets influenced by nanodisperse MnO_2 water suspension at oral introduction, just as at inhalation one [21, 26]. In case of oral introduction it can be determined by apparent ability of nanodisperse MnO_2 particles to penetrate into blood from gastrointestinal tract. MnO_2 nanoparticles reach brain tissues coming from bloodstream through capillary endothelial cells of blood brain barrier and accumulate in astrocytes [26]. Damaged astrocytes due to enhanced peroxidation of cells membranes lipids and active oxygen forms occurrence can lose their ability to capture and neutralize excessive quantities of "exciting" amino acid, namely glutamate; thus, excitotoxic effect evolves [43]. It becomes apparent as glutamate concentration in blood serum grows and GABA content in it decreases.

Morphological changes in brain tissues prove pathogenetic impact exerted by MnO_2 nanoparticles which was detected in the process of biochemical parameters assessment. Degenerative changes evolvement can be caused by direct oxidative

influence which nanoparticles have on neurons, glia cells, and vessels endothelium. The detected effects can only result from direct contact between nanoparticles and brain tissues which is the evidence of probable penetration through blood-brain barrier. The results of examining morphologic changes in brain tissues of Wistar rats, which were obtained at sub-acute intragastric introduction of nanodispersed MnO_2, enrich the existing data at sub-chronic intragastric introduction of MnO_2 nanoparticles, obtained by other authors. When MnO_2 nanoparticles are once a day introduced into rats' bodies orally during 28 days they are absorbed, accumulated in tissues after exposure and reveal their toxicity in doses lower than in case of micro-disperse analog [44].

Some authors present data showing that chronic effects exerted by MnO_2 nanoparticles lead to its accumulation in liver tissues with their consequent damage [45]. Histopathologic examinations revealed that MnO_2 nanoparticles had toxic influence on liver and kidneys [46]. There is an assumption that manganese is transported to organs with significant mitochondria content (to liver, pancreas and hypophysis in particular) where it is accumulated very fast [47].

Thus, the research revealed that nanodisperse MnO_2 water suspension, when being introduced daily into Wistar rats via gastric tube in doses equal to 260, 50, 10 mg/kg of body weight/a day during 90 days, causes lipid peroxidation activation (higher levels of lipid hydroperoxides and malonic dialdehyde in blood serum), and decrease in antioxidation system activity (lower OAS and Cu/Zn-SOD concentrations in blood serum). MnO_2 nanoparticles damage neurons and astrocytes membranes and lead to improper neurotransmitters ratio (higher glutamate concentration and lower GABA in blood serum). Pathomorphologic brain disorders occurred, such as vessels hyperemia, subarachnoid hemorrhages, brain edema with perivascular and pericellular spaces dilatation, focuses of nerve fibers demyelinization, focal dystrophic changes in vessels endothelium.

When a dose of nanodisperse MnO_2 water suspension was equal to 5 mg/kg of body weight/a day the substance did not exert any toxic effects.

Studying chronic toxicity of nanodisperse MnO_2 water suspension at intragastric introduction via gastric tube: toxicity of nanodisperse MnO_2 water suspension was examined at intragastric introduction via gastric tube under chronic experiment conditions; the examination was accomplished in full conformity with Methodical guidelines on toxicological-hygienic assessment of nanomaterial safety and Methodical guidelines on assessment order when assessing toxic effects exerted by nanomaterials on laboratory animals [48, 49].

To examine chronic toxicity of nanodisperse MnO_2 water suspension, a comprehensive experiment was performed on white male Wistar rats with body weight equal to 90 ± 5 g (n = 360). specific and integral parameters of negative effects in target organs were studied at daily intragastric introduction of nanodisperse MnO_2 water suspension via gastric tube. The experiment lasted for 180 days. The tested substance was daily introduced intragastrically via gastric tube, one time a day, the interval between introductions amounted to 24 hours. Mn concentration in water suspension in terms of MnO_2 was determined it amounted to 41.37 ± 2.5 mg/cm^3. Nanodisperse MnO_2 water suspension was introduced in the following doses: group 1–2.5 mg/kg (1/1000 LD_{50}); group 2–0.25 mg/kg (1/10,000 LD_{50}); group 3–0.05 mg/kg (1/50,000 LD_{50}[3]); group 4 (control one)—distilled water in volume equal. The substance concentration in the suspension was controlled weekly. There were several assessments of animals' overall health state, their survival rate, and body weight dynamics; these assessments took place just before the experiment beginning, then on the 30th day, 60th day, 90th day, 120th day, 150th day, and 180th day of the experiment. Blood samples were taken from animals of all groups out of a caudal vein; biochemical and hematologic parameters were detected before the experiment beginning, on the 30th day and on the 180th day.

The authors selected parameters for assessing animals body responses at chronic introduction of the tested substance in accordance with Methodical guidelines on toxicological-hygienic assessment of nanomaterial safety [48]. Animals were taken out of the experiment on the 180th day via sparing euthanasia with carbon dioxide. After euthanasia they were autopsied, and microscopic assessment of morphological changes in internal organs followed. Nanodisperse MnO_2 particles were identified in blood of experimental animals at intragastric introduction via gastric tube on the 180th day of the experiment.

The obtained results revealed that hair state, motion activity, food consumption, and body weight of experimental animals in experimental groups did not have any discrepancies with the same parameters in the control group during the whole experiment. Body weight dynamics of animals from experimental groups did not differ authentically from body weight dynamics of animals from control group. There were no deaths of experimental animals in experiment and control groups at introduction of nanodisperse MnO_2water suspension during the whole observation period.

Basing on the analysis of changes in hematologic and biochemical blood parameters of Wistar rats from groups 1 and 2 against group 4, the following negative effects, which characterize toxicity of nanosized MnO_2 water suspension, were highlighted:

1. *Oxidizing-antioxidant balance:* lipid peroxidation activation was detected as per lipid hydroperoxide growth in blood serum and MDA growth in blood plasma. Lipid hydroperoxide concentration in blood serum of experimental animals grew on the 30th day of the experiment; it grew 2.5 times in group 1 and 1.6 times in group 2 in comparison with the same parameter in group 4. On the 180th day of the experiment, these parameters were 2.0 and 1.7 times higher in comparison with the group 4 ($p = 0.001–0.003$). Increased MDA content was detected in experimental animals from group 1 and 2 on the 30th day of the experiment, and it was 1.9 times higher than in group 4 ($p = 0.001–0.002$). This parameter was at the same level as in group 4 on the 180th day of the experiment. There was a decrease in antioxidation system activity. On the 30th day of the experiment, animals from group 1 had authentic 1.4 times lower activity of Cu/Zn-SOD than the same parameter in group 4. This parameter in animals from group 2 was 1.3 times lower than in group 4. On the 180th day of the experiment, Cu/Zn-SOD in animals from group 1 was 1.5 times lower; and in animals from group 2, 1.4 times lower ($p = 0.001–0.005$). Level of AOS in animals from group 1 was 4.7 times lower than in animals from group 4 on the 30th day of the experiment; the same parameter in group 2 was 5.9 times lower. On the 180th day, AOS in group 1 was 3.5 times lower; and in group 2, 4.1 times lower ($p = 0.001–0.002$). AOS and Cu/ZN-SOD parameters in group 3 corresponded to the same parameters in group 4 during the whole experiment.

2. *Neurotransmitter balance violation:* animals in group 1 had 1.4 times lower dopamine level in blood serum on the 30th day of the experiment; and animals in group 2, 1.7 times lower level than animals in group 4 ($p = 0.002$). On the 180th day of the experiment, dopamine decreased 1.7 times in group 1 and 1.9 times in group 2. By the 30th day of the experiment, there was an increase in glutamate level in blood serum in groups 1 and 2 in comparison with group 4; this parameter was 2.5 and 3.3 times higher correspondingly ($p = 0.0011$). By the 180th day of the experiment, glutamate level in group 1 was 1.9 times higher than in group 4 and 3.7 times higher in group 2 ($p = 0.001$). GABA level

in blood serum of animals from group 1 on the 20th day of the experiment was 1.3 times lower; and in group 2, 1.5 times lower than in group 4; this parameter in groups 1 and 2 was 2.2 times lower than in group 4 on the 180th day of the experiment ($p = 0.0011$). There were not any authentic changes in these parameters in animals from group 3.

3. *Inflammatory effect:* inflammatory effect was detected in groups 1 and 2 as per 1.6 times increase in CRP level on the 30th day of the experiment; on the 180th day, it was 1.9 times higher than in control group ($p = 0.001–0.002$). Animals from group 1 had higher TNF on the 30th day of the experiment (5.5 times higher), and animals from group 2, 6.8 times higher in comparison with the same parameter in group 4 ($p = 0.001$). On the 180th day of the experiment, TNF increased 4.4 times in group 1 and 5.4 times in group 2.

4. *Insufficiency of bowels brush border epithelium:* lower activity of β-galactosidase in blood serum may indicate that insufficiency of brush border epithelium in bowels evolves. This parameter was 3.9 times lower in group 1 and 2.9 times lower in group 2 in comparison with group 4 on the 180th day of the experiment ($p = 0.001$). There were not any changes in this parameter in group 3 against the control level.

5. *Electrolyte balance violation* electrolyte balance violation was detected in group 1 as there was an authentic decrease in K level in blood serum on the 180th day. The level was 1.3 times lower than the same parameter level in group 4 ($p = 0.011$).

6. *Sensitization:* sensitization occurrence was detected as per EO increase in blood on the 30th day of the experiment. It grew 1.8 times in group 1 and 1.9 times in group 2 in comparison with this parameter level in group 4 ($p = 0.013–0.026$). EO-LY level increased 1.3–1.7 times and 1.3 times against the control parameter ($p = 0.001–0.036$). MO level decreased 1.6 times in group 1 on the 30th day; later this parameter grew 1.5 times on the 180th day ($p = 0.006–0.023$). Sensitization in animals from groups 1 and 2 remained on the 180th day as MO quantity increased 1.4–1.45 times, NE quantity decreased 1.5–1.7 times, and EO quantity decreased 3.7–5.1 times against group 4 ($p = 0.001–0.016$). There were not any authentic changes in the examined parameters in group 3 in comparison with control group during the whole experiment. As the remaining biochemical parameters were assessed, no authentic discrepancies were revealed between experimental groups and control group.

No authentic changes in the examined parameters were detected against the control group when nanodisperse MnO_2 water suspension was introduced in a dose equal to 0.05 mg/kg during 180 days. Electronic microscopy of animals' whole blood did not reveal any nanodisperse particles in blood of animals from group 4. X-ray spectrometry analysis did not reveal any Mn particles either (**Figure 15**). When nanodisperse MnO_2 water suspension was introduced intragastrically via gastric tube into Wistar rates in a dose equal to 0.25 mg/kg (1/10,000 LD_{50}) during 180 days there were bunches of particles which were ellipsoid-shaped and needle-shaped on electronic images. There were not any such particles in blood of rats from the control group (**Figure 16**). The size of these particles lies within 90–130 nm range, and it can be determined by their agglomeration.

In spite of the fact that X-ray spectrometry analysis did not reveal any Mn content in blood of experimental animals, which received a dose equal to 0.25 mg/kg (and it can be due to spatial resolution inaccuracy of this technique), visualized particles were considered to be Mn nanosized particles as they are identical with the pure suspension sample of the tested substance and are not detected in blood of animals from the control group.

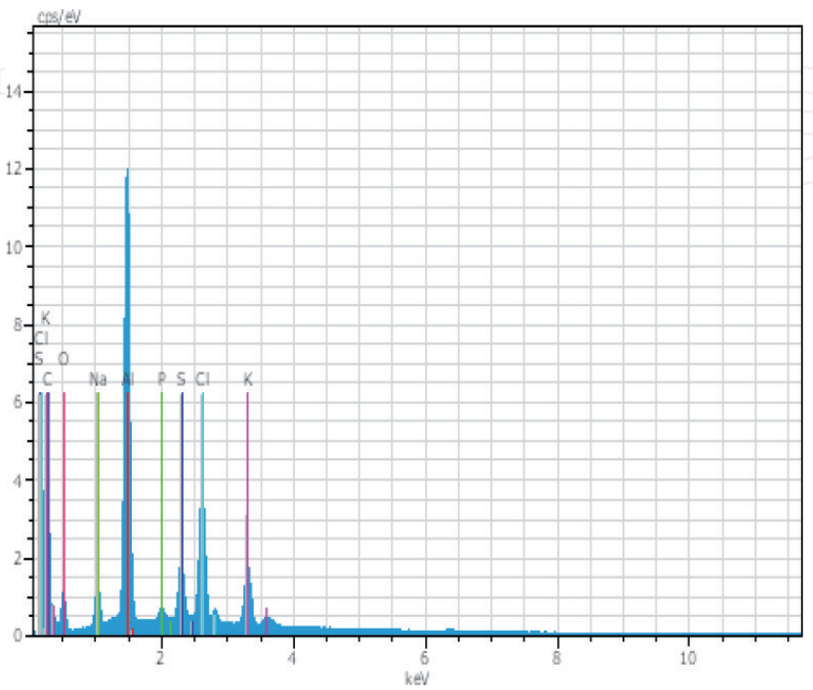

Figure 15.
X-ray spectrometry analysis of whole blood taken from a male Wistar rat form the control group [50].

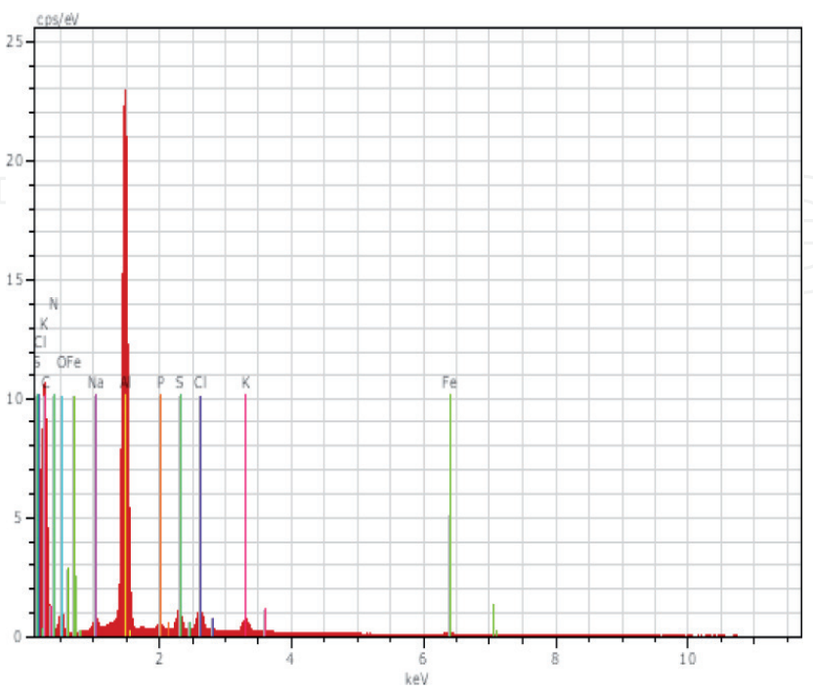

Figure 16.
X-ray spectrometry analysis of whole blood taken from an experimental animal, which received nanodisperse MnO_2 in a dose equal to 0.25 mg/kg [50].

4. Examining and assessing potential reproductive and mutagenic toxicity of nanodisperse manganese oxide water suspension at oral introduction with water

Embryotoxicity means capability of a chemical to exert negative influence on offspring during the initial period of pregnancy, i.e., the period between conception and embryo formation. Teratogenicity means capability of a chemical to cause malformations and deviations in offspring postnatal development when a female body is exposed to this chemical during pregnancy [51].

Embryotoxic and teratogenic effects exerted by nanodisperse MnO_2 were examined and assessed at oral introduction with water in accordance with methodical guidelines on studying embryotoxic effects of chemicals at hygienic validation of their maximum permissible concentration in water of water objects [52]. The experiment was performed on white senior male and female Wistar rats with body weight equal to 200 ± 10 g (n = 90). All the animals before the experiment underwent 14-day quarantine and were placed in standard cages made of polypropylene, two animals in each. Rats were divided into three groups, 15 animals in each. Groups 1 and 2 were experimental ones, and group 3 was a control one. To get female rats pregnant, intact male rats and intact female rats were made to mate under control conditions during two estrous cycles. The day of sperm detection in vaginal smear of a female rat via microscopy was thought to be the first day of pregnancy. Nanodisperse MnO_2 water suspension was introduced into pregnant female rats daily one time a day via gastric tube from the first to the twenty-first pregnancy day in two doses: 2.50 mg/kg (1/1000 LD_{50}) and 0.25 mg/kg (1/10,000 LD_{50}). Control group of rats received distilled water. Changes in general condition and behavior of experimental animals were registered during the whole experiment. Rat's body weight was measured on the first, eighth, fourteenth and twenty-first day of pregnancy. Rats were taken out of the experiment via sparing euthanasia with carbon dioxide on the twenty-first day of pregnancy. Pregnant female rats were dissected just after euthanasia. Assessment was performed in two stages. On the first stage, overall disorders in fetus development (embryotoxicity) were assessed. On the second stage, the focus was on occurrence of congenital malformations in internal organs and skeletal system of fetuses (teratogenicity).

The experiment results showed that pregnant female rats from groups 1 and 2 had ordinary motion activity during the observation period. Innate reflexes and reactions to external irritants were normal and rats ate their forage willingly. Their fur was clean, shiny, and smooth. Visible mucous tunics were physiologically colored without any discharge. Appearance, behavior, and body weight dynamics of rats from experimental groups did not have any authentic discrepancies from the same parameters of rats from control group during the whole observation period. There were not any signs of animals intoxication or death in both experimental groups during the whole observation period. The examination results showed that all the embryotoxicity parameters (number of implantation points, number of viable fetuses, and number of resorptions) of pregnant female rats receiving nanodisperse MnO_2 water suspension via gastric tube formed during first to twenty-first day of pregnancy in doses equal to 2.5 and 0.25 mg/kg had no authentic discrepancies with the same parameters of rats from control group ($p > 0.05$). Fetuses from each litter did not have any visible external congenital malformations when being examined externally. There were not any authentic discrepancies between body weight or cranio-caudal body dimensions of fetuses from experimental and control groups.

There were no morphologic changes in internal organs or skeletal system of fetuses from groups 1 and 2 at intragastric introduction of nanodisperse MnO_2

water suspension into Wistar rats from first to twenty-first day of pregnancy; there were no discrepancies between morphologic characteristics of fetuses internal organs and fetuses skeletal system between experimental and control groups. Fetuses from experimental groups and control group had multilayer flat epidermis with increased number of layers up to eight cells; derma cells were spindle-shaped; fibers were tightly located and had numerous hair follicles. Subcutaneous fatty tissue was in the form of sporadic small lipocyte bunches (**Figure 17**). Small intestine wall is fully formed; limbic epithelium has characteristic appearance; Paneth cells are large and located not only in crypts bottom area, but also in villi epithelium. Beaker cells are sporadic (**Figure 18**).

Cartilaginous elements are mature; eosinophilic intracellular substance prevails in most cartilages (**Figures 19** and **20**).

There were numerous focuses of indirect and direct osteogenesis. Skeletal muscles are with small diameter of fibers and banding that is not clearly visible. Brain hemispheres cortex is cellular, layers are poorly differentiated and prevail over medulla. Cardiac histiocytes are with small section and large nucleuses. Fibers are spongy. Connective tissue content in cardiac muscle is minimal. Banding is not detected. Marrow is cellular; its bulk is represented by cells of erythropoetic type; there are no lipocytes.

Examining and assessing mutagenic activity of nanodisperse MnO_2 water suspension at oral introduction with water: micronucleus test is a widespread technique applied for assessing mutagenic activity of new unknown chemicals; the test was independently worked out and implemented by Heddle and Schmid in early 1970s [53]. Micronucleuses are small DNA-containing formations consisting of acentric chromosome fragments. During telophase, these fragments can become a part of daughter cells nucleuses or form singular or numerous micronucleuses in cytoplasm. The test is based on microscopic detection of cells with micronucleuses. Spontaneous frequency of cells with micronucleuses amounts to 0.1–0.2% [54].

Data on mutagenic activity, which nanosized MnO_2 particles, may be contradictory. The authors have not been able to find any research works proving apparent mutagenic properties of MnO_2 nanoparticles. At the same time, some experts state that MnO_2 nanoparticles are undoubtedly genotoxic "in vivo" [55]. There are data given by a number of researchers that manganese nanoparticles (52.1 ± 23.8 nm) at 24-hour exposure on PC-12 cells in concentration equal to 10 mg/cm^3 are able to inhibit PARK2 gene and tyrosine hydroxylase gene expression (The latter is an enzyme that catalyzes the first limiting stage of catecholamines synthesis, including dopamine.) It is detected that manganese nanoparticles enhance SNCA gene

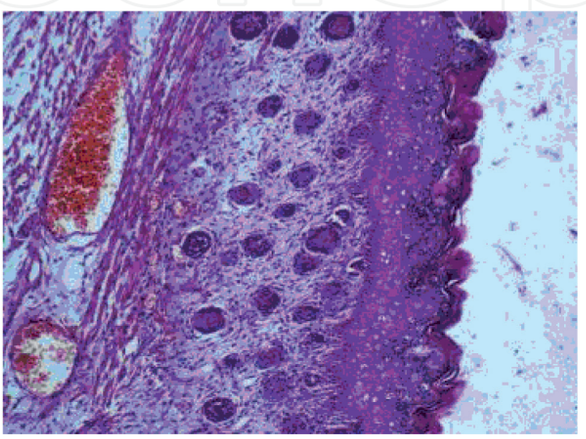

Figure 17.
Epidermis of Wistar rat fetus on the twenty-first day of pregnancy at intragastric introduction of nanodisperse MnO_2 water suspension via gastric tube. Painted with hematoxylin-eosin, magnification ×200 [10].

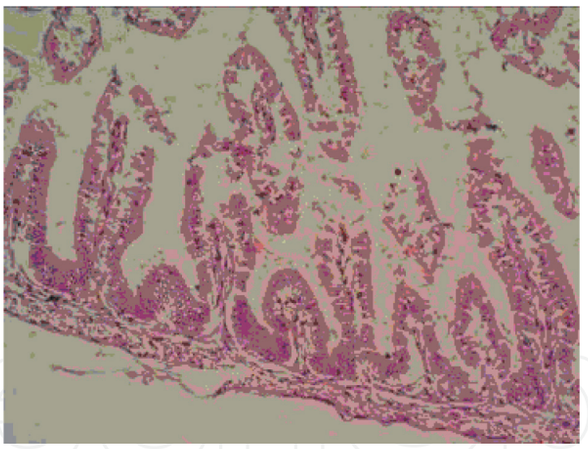

Figure 18.
Small intestine of a Wistar rat fetus on the twenty-first day of pregnancy at intragastric introduction of nanodisperse MnO_2 water suspension via gastric tube. Painted with hematoxylin-eosin, magnification ×200 [10].

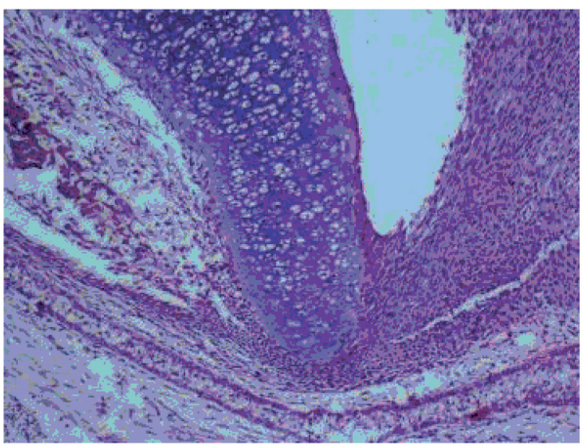

Figure 19.
Brainpan and brain of a Wistar rat fetus on the twenty-first day of pregnancy at intragastric introduction of nanodisperse MnO_2 water suspension via gastric tube. Painted with hematoxylin-eosin, magnification ×200 [10].

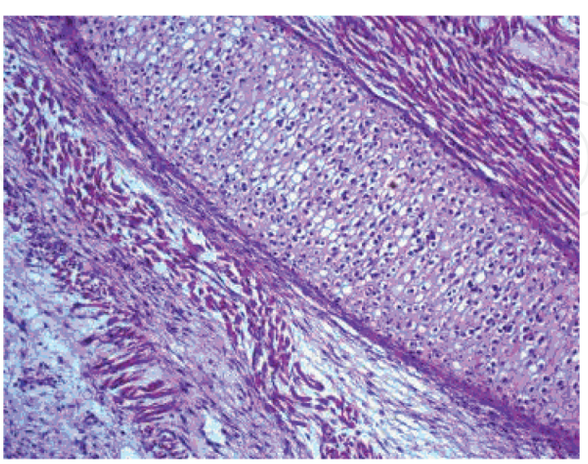

Figure 20.
Ribs and intercostal muscles of a Wistar rat fetus on the twenty-first day of pregnancy at intragastric introduction of nanodisperse MnO_2 water suspension via gastric tube. Painted with hematoxylin-eosin, magnification ×200 [10].

expression, which makes α-synucleins double in cells participating in various neurodegenerating disorders evolvement. After nanodisperse, MnO_2 was orally introduced into Wistar rats in doses equal to 300 and 1000 mg/kg during 28 days; there

was an increased number of DNA damages in leucocytes, and also an increased number of micronucleuses and chromosome aberrations in marrow cells.

Potential mutagenic activity of nanodisperse MnO_2 water suspension in polychromatocytes (reticulocytes) of mammals marrow was assessed via micronucleus test [53]. The experiment was carried out on C57B1/6 white male mice with body weight equal to 20.0 ± 1.0 g (n = 24). The experiment lasted for 2 days. Experimental animals were divided into four groups (six animals in each); groups 1 and 2 were experimental ones, group 3 was negative control, and group 4 was positive control. Nanodisperse MnO_2 water suspension was once introduced via gastric tube in two doses: group 1 received 10.3 mg/kg (1/250 LD_{50}), group 2–5.15 mg/kg dose (1/500 LD_{50}), and group 3 (negative control)—distilled water in a volume equal to 0.2 cm^3 group 4 (positive control)—cyclophosphamide water suspension was once introduced intraperitoneally into mice from in a dose equal to 20 mg/kg in a volume equal to 0.2 cm^3. Cyclophosphamide is known to be cytogenetically active [13].

Thus, nanodisperse MnO_2 water suspension at a single intragastric introduction via gastric tube into C57B1/6 male mice in doses equal to 10.3 and 5.15 mg/kg does not cause increased micronucleuses formation in vivo and, consequently, does not have any mutagenic effects. As per other authors' data, there is no information on possible penetration of MnO_2 nanoparticles into cells nucleuses. It reduces the risk of direct contact between examined particles and cellular DNA [23]. DNA damage can occur through activation of lipid peroxidation and excessive AOF production from damaged membranes, which leads to cytokines induction (TNF-a tumor necrosis factor) and DNA damage. It can result in transcription factors activation, NF-KB in particular, which is responsible for polygenic expression. As a result, apoptotic mechanism is activated, or programmed cells death is inhibited, which can cause tumor activity [56, 57]. Some authors state that manganese nanoparticles (52.1 ± 23.8 nm) when exerting a 24-hour effect on PC-12 cells in concentration equal to 10 mg/cm^3 are able to inhibit PARK2 gene expression and gene of tyrosine hydroxylase (an enzyme that catalyzes the first limiting stage of catecholamine synthesis, dopamine included). It is proved that manganese nanoparticles enhance SNCA gene expression which leads to double increase in α-synucleins in cells taking part in evolvement of various neurodegenerating disorders. When nanodisperse MnO_2 was introduced into Wistar rats orally in doses equal to 300 and 1000 mg/kg during 28 days DNA damages in leucocytes increased, a number of micronucleuses and chromosome aberrations in marrow cells grew. These changes were accompanied with inhibition of various ATPases activity; here changes in ALAT, ASAT, and LDG activity in liver, kidneys, and blood serum were dose depending [44]. We could not find any research proving apparent mutagenic properties of MnO_2 particles. At the same time, a number of authors showed that MnO_2 nanoparticles had evident genotoxicity "in vivo" [43].

Examining and assessing gonadotoxic activity (screening) of MnO_2 oxide water suspension at oral introduction with water: gonadotoxicity of nanodisperse MnO_2 water suspension was examined on laboratory animals under subchronic experiment conditions in accordance with guidelines 2492-81 "On studying chemicals gonadotoxicity at hygienic standardization in water of water reservoirs" and international recommendations [58, 59]. The authors examined gonads of white male Wistar rats with body weight equal to 190 ± 20 g (n = 40). Experimental animals were divided into five groups, eight animals in each. Water suspension containing nanodisperse MnO_2 was introduced in a concentration equal to 36.0 ± 2.3 mg/cm^3, into animals from experimental groups via gastric tube once a day every day in following doses: group 1 received 257.7 mg/kg (1/10 LD_{50}), group 2–51.54 mg/kg (1/50 LD_{50}), group 3–10.3 mg/kg (1/250 LD_{50}),

group 4–5.15 mg/kg (1/500 LD_{50}), and group 5 (control)—distilled water in a volume equal. The experiment lasted for 90 days. Animals euthanasia was accomplished with carbon dioxide. Then, a special instrument was applied to take out epididymis and make a longitudinal cut along it. Extraction of the epididymis in 10 cm^3 of 0.9% NaCl solution was performed during 2 minutes at room temperature being 22°C. Sperm quantity was calculated in Goryaev chamber. Specimens microscopy was performed with the use of MC 100X microscope (Micros, Austria). The task was to assess such functional and morphometric parameters as sperm mass, total sperm quantity, number of alive sperm, sperm mobility duration, osmotic and acidic resistance of sperm, relative quantity of sperm pathologies.

The obtained results revealed authentic 2.18 times decrease in sperm quantity in male rats from group 1 against the control group ($p < 0.05$). Male rats from group 2 had authentically 1.7 times lower quantity of sperm than rats from the control group. There were no authentic discrepancies in sperm number between male rats from groups 3, 4 and 5 and the control group. There was an authentic 1.2–1.3 times decrease in osmotic and acidic resistance of sperm in rats from groups 1 and 2 against the control group parameter ($p < 0.05$). There were no discrepancies in this parameter in rats from groups 3, 4 and 5 and the control group. Such morphological changes as sperm head, tail, and neck pathology occurred in groups 1 and 2 1.7–10.3 times more frequently than in the control group (**Figures 21** and **22**). This parameter in groups 3, 4, and 5 did not have any discrepancies with the control group parameter.

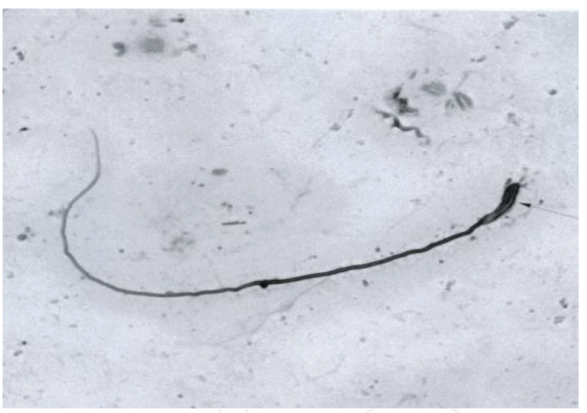

Figure 21.
A spermatozoon neck pathology in a male Wistar rat at oral introduction of nanodisperse MnO_2 in a dose equal to 51.54 mg/kg, magnification ×100 [55].

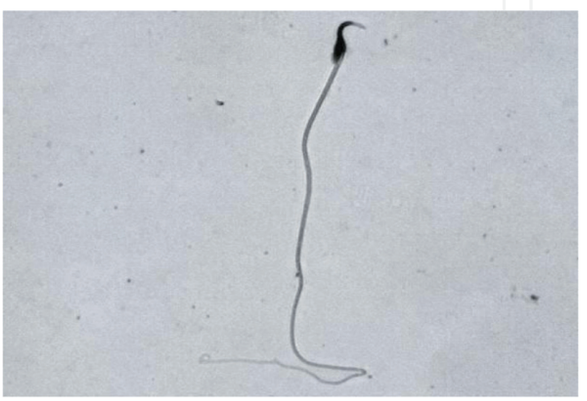

Figure 22.
A spermatozoon neck and head pathology in a male Wistar rat at oral introduction of nanodisperse MnO_2 in a dose equal to 257.7 mg/kg, magnification ×200 [55].

Therefore, nanodisperse MnO_2 water suspension does not exert any gonadotoxic effects on male Wistar rats when it is introduced into them via gastric tube during 90 days in doses equal to 10.3–5.15 mg/kg.

5. Conclusion

Contemporary research in nanotoxicology calls for studying and systemizing miscellaneous toxic effects exerted by new nanomaterials at various introduction ways and exposure period. Special attention is paid to determining target organs and negative effects caused by nanoparticles impacts, which do not occur after exposure to analog microparticles. To obtain comprehensive characteristics, one should study remote toxic effects such as embryotoxicity, gonadotoxicity, mutagenic activity occurrence, etc.

The authors conducted experimental research of nanodisperse MnO_2 water suspension at intragastric, inhalation, and skin-resorptive introduction into small rodents (mice and Wistar rats) with various exposure periods. It allowed to obtain a sufficiently profound and detailed characteristics of the toxic effects exerted by this substance, to determine the target organs and to reveal dose-dependent effects.

The obtained knowledge provides better understanding of toxic impact exerted by nanosized metal oxides, which have great potential of application in human activities. It is vital for working out efficient measures aimed at providing safety in production processes and in nanomaterials application.

Acknowledgements

The authors are grateful to specialists working at the multiphase disperse system laboratory of Technical Chemistry Institute (the Russian Academy of Sciences, Urals Branch), specialists working at Chemical Technologies Department of Perm National Research Polytechnic University, specialists working at Human Ecology and Life Activity Safety Department of Perm State National Research University, as they all contributed into providing data and materials for this edition.

Notation and abbreviations

IT	information technology
EU	European Union
SUN	sustainable nanotechnologies
GLP	good laboratory practice
XRD	X-ray diffraction
CAS	chemical abstracts service
IUPAC	International Union of Pure and Applied Chemistry
CTAB	cetyltrimethylammonium bromide
ILAR,	Institute for Laboratory Animal Research
DELS	division on earth and life studies
AOF	active oxygen forms
GSSG	oxidized glutathione form
GSH	reduced glutathione form
CL_{50}	concentration causing death of animals in quantity 50%
TCL_0	minimal toxic concentration
LDL_0	minimal lethal dose

LD_{50}	dose causing death of animals in quantity 50%
TL_{50}	time causing death of animals in quantity 50%
GABA	γ-aminobutyric acid
LP	lipid peroxidation
MDA	malonic dialdehyde
Cu/Zn-SOD	Cu/Zn-superoxide dismutase
OAS	overall antioxidant state
DNA	deoxyribonucleic acid

Author details

Nina Vladimirovna Zaitseva and Marina Alexandrovna Zemlyanova*
FBSI "Federal Scientific Center for Medical and Preventive Health Risk Management Technologies", Perm, Russian

*Address all correspondence to: zem@fcrisk.ru

References

[1] Nanoindustry Analysis Results in CU and EES (Analytical Material) [Internet]. 2014. Available from: www.nanonewsnet.ru/news/2015/rezultaty-analiza-nanoindustrii-v-ramkakh-ts-eep [Accessed: 10 December 2018]

[2] Nanotechnologies Market in Russia [Internet]. 2017. Available from: http://prnews.ru/topic/analiz-rynka-nanotehnologij-v-rossii [Accessed: 11 December 2018]

[3] Onishchenko G. Security strategy in nanoindustry. Population Health and Environment. 2011;**5**:4-8

[4] Risk Assessment of Products of Nanotechnologies [Internet]. 2009. Available from: http://ec.europa.eu/health/ph_risk/committees/04_scenihr/docs/scenihr_o_023.pdf [Accessed: 11 December 2018]

[5] About Manganese [Internet]. 2017. Available from: https://www.americanelements.com/mn.html [Accessed: 11 December 2018]

[6] Portable Power Source [Internet]. 2009. Available from: http://bd.patent.su/2396000-2396999/pat/servl/servlet9ef1.html [Accessed: 11 December 2018]

[7] Dontsova EA, Budashov IA, Eremenko AV, Kurochkin IN. Hydrogen peroxide-sensitive amperometric sensor based on manganese dioxide nanoparticles. Nanotechnologies in Russia. 2008;**3**(7-8):510-520. DOI: 10.1134/s199507800807015x

[8] Detection of Nanomaterials which can be Potentially Dangerous for Human Health. MU 1.2.2522-09 [Internet]. 2009. Available from: www.gostrf.com/normadata/1/4293828/4293828130.pdf [Accessed: 11 December 2018]

[9] Sinha K, Suzuki K, Takahara M, Azuma H, Nonaka T, Fukumoto K. Mesostructured manganese oxide/gold nanoparticle composites for extensive air purification. Angewandte Chemie International. 2007;**46**:2891-2894. DOI: 10.1002/ange.200605048

[10] Zvezdin V, Zemlyanova M, Akafieva T. Inhalation toxicity of nanodispersed manganese oxide aerosol. Occupational Health and Industrial Ecology. 2015;**12**:13-16

[11] Guide for the Care and Use of Laboratory Animals. 8th ed. Washington: The National Academies Press; 2011. 220 p

[12] Manganese [Internet]. 2017. Available from: https://chem.libretexts.org/Textbook_Maps/Analytical_Chemistry/Supplemental_Modules_%28Analytical_Chemistry%29/Analytical_Chemiluminescence/2%3A_Chemiluminescence_Reagents/2.07%3A_Manganese [Accessed: 10 December 2018]

[13] Greg S, Singh K. Adsorption, Surface Area, Porosity. Moscow: Mir; 1984. 306 p

[14] Barrett E, Joyner L, Halenda P. The determination of pore volume and area distributions in porous substances. I. Computations from nitrogen isotherms. Journal of the American Chemical Society. 1951;**7**:373-380. DOI: 10.1021/ja01145a126

[15] Zaitseva N, Zemlianova M, Zvezdin V, Akafieva T, Saenko E. Acute inhalation toxicity of manganese oxide nanoparticles. Nanotechnologies in Russia. 2015;**10**(5-6):468-474. DOI: 10.1134/S1995078015030180

[16] Whitesides G, Eigler D, Anders R, et al. Nanotechnology in the next decade. In: Roco MC, Williams RS, Alivisatosa P, editors. Forecast Research. Moscow: Mir; 2002. 292 p

[17] Meynen V, Cool P, Vansant E. Verified syntheses of mesoporous materials. Microporous and Mesoporous Materials. 2009;**125**:170-223. DOI: 10.1016/j.micromeso.2009.03.046

[18] Gyrdasova O, Krasil'nikov V, Bazuev G. Synthesis of micro- and nanosized manganese oxides from hydrated manganese oxalates and products of their chemical modification with ethylene glycol. Russian Journal of Inorganic Chemistry. 2009;**7**:1035-1040. DOI: 10.1134/S0036023609070080

[19] Lison D, Lardot C, Huaux F, Zanetti G, Fubini B. Influence of partice surface area on the toxicity of insoluble manganese dioxide dusts. Archives of Toxicology. 1997;**71**(12):725-729. DOI: 10.1007/s002040050453

[20] Frick R, Müller-Edenborn B, Schlicker A, Rothen-Rutishauser B. Comparison of manganese oxide nanoparticles and manganese sulfate with regard to oxidative stress, uptake and apoptosis in alveolar epithelial cells. Toxicology Letters. 2011;**205**:163-172. DOI: 10.1016/j.toxlet.2011.05.1037

[21] Stefanescu D, Khoshnan A, Patterson P, Hering J. Neurotoxicity of manganese oxide nanomaterials. Journal of Nanoparticle Research. 2009;**11**(8):1957-1969. DOI: 10.1007/s11051-008-9554-1

[22] Elder A, Gelein R, Silva V, Feikert T, Opanashuk L, Carter J, et al. Translocation of inhaled ultrafine manganese oxide particles to the central nervous system. Environmental Health Perspectives. 2006;**114**:1172-1178. DOI: 10.1289/ehp.9030

[23] Ostiguy C, Asselin P, Malo S, Nadeau D. Prse en charge du manganisme d'origine professionnelle: Consensus d'un groupe d'experts: Rapport IRSST, No 416. Montreal: IRSST; 2005. 62 p

[24] Ostiguy C, Malo S, Asselin P. Synthese des connaissances scientifiques sur les risques d'atteinte a la sante suite a une exposition professionnelle au manganese: rapport IRSST, No 339. Montreal: IRSST; 2003. 41 p

[25] Afeseh Ngwa H, Kanthasamy A, Gu Y, Fang N. Manganese nanoparticle activates mitochondrial dependent apoptotic signaling and autophagy in dopaminergic neuronal cells. Toxicology and Applied Pharmacology. 2011;**256**:227-240. DOI: 10.1016/j.taap.2011.07.018

[26] Horváth E, Máté Z, Takács S, Pusztai P, Sápi A, Kónya Z, et al. General and electrophysiological toxic effects of manganese in rats following subacute Administration in Dissolved and Nanoparticle Form. The Scientific World Journal. 2012:1-7. DOI: 10.1100/2012(6)/520632

[27] Crittenden P, Filipov N. Manganese-induced potentiation of in vitro pro-inflammatory cytokine production by activated microglial cells is associated with persistent activation of p38 MAPK. Toxicology in Vitro. 2008;**22**: 18-27. DOI: 10.1016/j.tiv.2007.07.004

[28] Sárközi L, Horváth E, Kónya Z, Kiricsi I. Subacute intratracheal exposure of rats to manganese nanoparticles: Behavioral, electrophysiological, and general toxicological effects. Inhalation Toxicology. 2009;**1**:83-91. DOI: 10.1080/08958370902939406

[29] Wang J, Rahman M, Duhart H, Newport G. Expression changes of dopaminergic system-related genes in PC12 cells induced by manganese, silver, or copper nanoparticles. Neurotoxicology. 2009;**30**:926-933. DOI: 10.1016/j.neuro.2009.09.005

[30] Oberdorster G, Sharp Z, Atudorei V. Translocation of inhaled ultrafine particles to the brain. Inhalation

Toxicology. 2004;**16**:437-445. DOI: 10.1080/08958370490439597

[31] Nanotechnology KJ. Piecing together the puzzle of risk. Controversies in Science and Technology. 2011;**3**:243-255. DOI: 10.1089/9781934854204.243

[32] Laohaudomchok W, Lin X, Herrick RF, Fang SC, Cavallari JM, Shrairman R, et al. Neuropsychological effects of low-level manganese exposure in welders. Neurotoxicology. 2011;**32**(2):171-179. DOI: 10.1016/j.neuro.2010.12.014

[33] Li T, Shi T, Li X, Zeng S, Yin L, Pu Y. Effects of nano-MnO_2 on dopaminergic neurons and the spatial learning capability of rats. International Journal of Environmental Research and Public Health. 2014;**11**(8):7918-7930. DOI: 10.3390/ijerph110807918

[34] Zemlyanova M, Zvezdin V, Akafieva T. Inhalation toxicity of nanodispersed manganese oxide aerosol. Labor Medicine and Industrial Ecology. 2015;**12**:13-17

[35] Amatucci GG, Pereira N. Fluoride based electrode materials for advanced energy storage devices. Journal of Fluorine Chemistry. 2007;**128**:243-262. DOI: 10.1016/j.jfluchem.2006.11.016

[36] Hua M, Zhang S, Pan B, Zhang W, Lv L, Zhang Q. Heavy metal removal from water/wastewater by nanosized metal oxides: A review. Journal of Hazardous Materials. 2012;**211-212**:317-331. DOI: 10.1016/j.jhazmat.2011.10.016

[37] Zaitseva N, Zemlyanova M, Zvezdin V, Akafyeva T. Biological effects of manganese oxide nanoparticles after peroral intake. Journal of Pharmacy and Nutrition Sciences. 2013;**3**(4):231-237

[38] Zaitseva N, Zemlyanova M, Zvezdin V, Saenko E, Tarantin A, Makhmudov R, et al. Toxicological-hygienic assessment of nanodisperse and microdisperse manganese oxide safety (III, IV). Nutrition Issues. 2012;**81**(5):13-19

[39] Shtabskiy B. Quantitative assessment of cumulation. Hygiene and Sanitary. 1973;**8**:24-28

[40] Mousavi Z, Hassanpourezatti M, Najafizadeh P, Rezagholian S, Safi Rhamanifar M, Nosrati N. Effects of subcutaneous injection MnO_2 micro- and nanoparticles on blood glucose level and lipid profile in rat. The Iranian Journal of Medical Sciences. 2016;**41**(6):518-524

[41] Zaitseva N, Zemlyanova M, Zvezdin V, Akafyeva T, Mazunina D, Dovbyish A. Effects of subchronic exposure manganese oxide nanoparticles on the central nervous system, lipid peroxidation and antioxidant enzymes in rats. Health Risk Analysis. 2014;**4**:66-77

[42] Sakon S, Xue X, Takekawa M, Sasazuki T, Okazaki T, Kojima Y, et al. NF-kB inhibits TNF-induced accumulation of ROS that mediate prolonged MAPK activation and necrotic cell death. The EMBO Journal. 2003;**22**(15):3898-3909. DOI: 10.1093/emboj/cdg379

[43] Tin-Tin W-S, Fujimaki H. Nanoparticles and neurotoxicity. Journal of Molecular Science. 2011;**12**:6267-6280. DOI: 10.3390/ijms12096267

[44] Singh SP, Kumari M, Kumari SI, Rahman MF. Toxicity assessment of manganese oxide micro and nanoparticles in Wistar rats after 28 days of repeated oral exposure. Journal of Applied Toxicology. 2013;**33**(10):1165-1179. DOI: 10.1002/jat.2887

[45] Mousavi Z, Hassanpourezatti M, Najafizadeh P, Rezagholian S, Rhamanifar NN. Effects of subcutaneous injection MnO_2 micro- and nanoparticles on blood glucose level and lipid profile in rat. Iranian Journal of Medical Sciences. 2016;**41**(6):518-524

[46] Ghaedi S, Hassanpour-Ezatti M, Naji T, Rahmanifar MS. Comparison of tissue damages resulting from chronic administration of manganese dioxide nano-and microparticles on the liver, kidneys and testes of rats. Modares Journal of Medical Sciences: Pathobiology. 2014;**16**(4):67-81

[47] Deng Q, Liu J, Li Q, Ket C, Liu Z, Shen Y, et al. Interaction of occupational manganese exposure and alcohol drinking aggravates the increase of liver enzyme concentrations from a cross-sectional study in China. Environmental Health. 2013;**12**:30. DOI: 10.1186/1476-069X-12-30

[48] Onishhenko GG, Tutel'jan VA, Hotimchenko SA, Gmoshinskij IV, et al. Toxicologic-Hygienic Assessment of Nanomaterial Safety: MU 1.2.2520-09. Moscow: Federal Center for Hygiene and Epidemiology of Rospotrebnadzor; 2009. 43 p

[49] Onishhenko GG, Bragina IV, Aksenova OI, Zavistjaeva TJu, Assessment et al. Order when Assessing Toxic Effects Exerted by Nanomaterials on Laboratory Animals. MU1.2.2869-11. Moscow: Federal center for Hygiene and Epidemiology of Rospotrebnadzor; 2011. 23 p

[50] Zaitseva N, Zemlyanova M, Zvezdin V, Sayenko Y. Toxicological and hygienic safety assessment of the aqueous suspension of nano-dispersed silicon dioxide, synthesized using liquid-crystal templating. Health Risk Analysis. 2013;**1**:65-72

[51] Sanockij I, Sidorov K, editors. Russian Glossary of Selected Terms from Preventive Toxicology. Moscow: Centr mezhdunar. proektov GKNT; 1982. 68 p

[52] Methodical Guidelines on Studying Embryotoxic Effects of Chemicals at Hygienic Validation of their Maximum Permissible Concentration in Water of Water Objects. MU 2926-83. [Internet]. 1983. Available from: http://www.normacs.ru/Doclist/doc/11NEJ.html [Accessed: 11 December 2018]

[53] Ledebur MV, Schmid W. The micronucleus test methodological aspects. Mutation Research/Fundamental and Molecular Mechanisms of Mutagenesis. 1973;**19**(1):109-117. DOI: 10.1016/0027-5107(73)90118-8

[54] Manual on experimental (preclinical) study of new pharmacological substances. Edited by a corresponding member of the RAMS, Prof. R.N. Habriev. Moscow: Methodical Guidelines; 2005. 832 p. Available from: https://elibrary.ru/item.asp?id=19116235&

[55] Minigalieva IA, Katsnelson BA, Privalova LI, Sutunkova MP, Gurvich VB, Shur VY, et al. Attenuation of combined nickel (II) oxide and manganese (II, III) oxide nanoparticles' adverse effects with a complex of bioprotectors. International Journal of Molecular Sciences. 2015;**16**(9):22555-22583. DOI: 10.3390/ijms160922555

[56] Pahl H. Activators and target genes of Rel/NF–kB transcription factors. Oncogene. 1999;**18**:6853-6866. DOI: 10.1038/sj.onc.1203239

[57] Takizawa H, Ohtoshi T, Kawasaki S, Kohyama T, Desaki M, Kasama T, et al. Diesel exhaust particles induce NF-kB activation in human bronchial epithelial cells in vitro: Importance in cytokine transcription. Journal of Immunology. 1999;**162**:4705-4711. DOI: 0022-1767/99/$02.00

[58] Guidelines for the Study Gonadotoxic Action of Chemical Substances in Hygienic Rationing

of Water Reservoirs. MU 2492-81 [Internet]. 1981. Available from: http://docs.cntd.ru/document/675400365 [Accessed: 11 December 2018]

[59] ICH Harmonised Tripartite Guideline [Internet]. 1993. Available from: https://www.ich.org/fileadmin/Public_Web_Site/ICH_Products/Guidelines/Efficacy/E7/Step4/E7_Guideline.pdf [Accessed: 11 December 2018]